IEEE Access
Multidisciplinary | Rapid Review | Open Access Journal

Received July 9, 2019, accepted July 28, 2019, date of publication August 2, 2019, date of current version August 30, 2019.

Digital Object Identifier 10.1109/ACCESS.2019.2932762

A Secure Wireless Information and Energy Cooperation Transmission Strategy in Spectrum Sharing Networks With Untrusted Dual-Relay

DAQIAN ZHAO, (Student Member, IEEE), HUI TIAN, (Senior Member, IEEE), AND PING ZHANG, (Fellow, IEEE)

State Key Laboratory of Networking and Switching Technology, Beijing University of Posts and Telecommunications, Beijing 100876, China

Corresponding author: Ping Zhang (pzhang@bupt.edu.cn)

This work was supported in part by the Science and Technology of the Winter Olympics under Grant 2018YFF0301201, and in part by the Funds for Creative Research Groups of China under Grant 61421061.

ABSTRACT Spectrum efficiency, energy efficiency, and physical layer security are three critical issues in designing wireless networks, such as an energy-constrained device-to-device (D2D) communication in secure spectrum sharing femtocell networks. In this paper, we investigate a problem of security cooperation transmission between a single-antenna primary system and a multi-antenna wireless-powered untrusted secondary system, where the untrusted secondary devices can be regarded as potential malicious decoders. A novel artificial noise-aided (AN-aided) joint time division- and power splitting-based three-phase secure wireless information and energy cooperation transmission strategy is proposed for spectrum sharing networks with untrusted cooperative dual-relay. Furthermore, we consider two scenarios that the untrusted secondary system knows perfect and imperfect channel state information (CSI). We focus on the design of time division ratios, power splitting ratios, and beamforming vectors, with the objective to maximize the data rate of the untrusted secondary system, subject to the target data rate requirement of the primary system and the untrusted secondary system's confidentiality constraints, energy harvesting requirements, and power consumption constraints. Simulation results demonstrate that our proposed strategy is the best and significantly improves the average data rate of the untrusted secondary system under different primary user target data rate requirements, primary transmitter rated transmit power, untrusted secondary user initial power, and primary transmitter power allocation ratios. Finally, a large number of simulations show that the time division ratios have a significant impact on the performance of the system, and these simulation results also verify the feasibility and effectiveness of the proposed strategy.

INDEX TERMS Spectrum sharing networks, energy harvesting, physical layer security, time division, power splitting.

I. INTRODUCTION

A. MOTIVATION

With the explosive growth of the number of wireless devices in recent years, the demand for spectrum resources has increased exponentially, and the spectrum scarcity issue has become more and more severely. In response to spectrum scarcity, spectrum sharing technology has been regarded as an effective solution to improve spectrum efficiency by allowing the secondary system to share the spectrum authorized to the primary system [1]. Spectrum sharing techniques can be classified into three categories generally: Interweave, underlay, and overlay [2], [3]. For interweave spectrum sharing, the secondary system can access spectrum holes opportunistically. For underlay spectrum sharing, the secondary transmitters (STs) can transmit signals simultaneously with the primary transmitters (PTs) under the constraint that the interference caused by the STs to the primary receivers must be below a predetermined threshold. For overlay spectrum sharing, which is a win-win cooperation strategy for both primary and secondary systems, the secondary system actively assists the primary user (PU) to forward its signal in exchange for permission to access the authorized spectrum in the time domain, frequency domain, or spatial domain.

The associate editor coordinating the review of this article and approving it for publication was Zhenhui Yuan.

Compared with interweave technique which refers to the opportunistic access scheme, cooperation strategy does not require the STs to sense spectrum holes for seeking the opportunities of the secondary communications. Compared with underlay technique which sets the limit on the interference to the primary system, cooperation strategy focuses on the end performance, such as the target data rate or signal-to-interference-plus-noise-ratio (SINR) of the PU, hence the STs are no longer restricted to transmit signals with low power.

However, information cooperation between primary and secondary systems is difficult when the STs are low energy devices rather than a powerful base station. Therefore, it is not enough to consider cooperation between primary and secondary systems only at the information level. Recently, harvesting energy from radio frequency (RF) signals are emerging as an attractive solution to power energy-constrained wireless devices [4]–[8]. Unlike conventional battery-powered communication devices, RF energy harvesting can provide a sustainable energy supply from a radio environment for energy-constrained wireless devices, such as internet of things devices, wireless sensor devices, small-scale machine type communication devices, and D2D communication devices. Consequently, powering energy-constrained wireless devices with RF energy can provide both spectrum efficiency and energy efficiency solution for overlay spectrum sharing networks.

Although information and energy cooperation can be more flexible and effective by exploiting energy-constrained wireless devices rather than energy-unconstrained conventional fixed relays, these unauthorized devices may be untrusted and might maliciously decode the confidential information from authorized users. Therefore, to cope with the threat to information security, physical layer security, as an efficient complementary technique for conventional information security mechanisms, has been widely recognized as a promising approach to enhance the security of wireless communications by only exploiting the characteristics of wireless channels, such as fading, noise, and interference [9]–[11]. Compared with the conventional cryptographic technique which has been plagued by increased signaling overhead and higher computational complexity, physical layer security has the advantages of lower computational complexity and resource saving. Consequently, this is a subject worthy of study that how to address secure wireless information and energy cooperation transmission issue for overlay spectrum sharing networks.

B. RELATED WORKS

In recent years, information and energy cooperation transmission [12]–[14] has aroused keen interest and has been widely investigated in cooperative cognitive radio networks (CRNs) [15]–[32]. The authors of [15] propose an information and energy cooperation scheme in CRNs. It is shown in [15] that the beamforming scheme with information and energy cooperation outperforms that without energy cooperation. In [16], the authors investigate an optimal cooperation strategy in CRNs, namely, the optimal decision (to cooperate with the PU or not) and the optimal action (to spend how much time on energy harvesting and to allocate how much power for cooperative relaying). Moreover, they further study the optimal action in cooperation and non-cooperation modes to maximize the achievable throughput of the secondary user (SU) and derive the optimal closed-form solutions. In [17]–[20], the authors study a problem of simultaneous wireless information and power transfer (SWIPT) in cooperative CRNs. In [21] and [22], the authors study the sum throughput maximization problem of information and energy cooperation in underlay- and overlay-based CRNs. In [23], a new wireless energy harvesting protocol is proposed in an underlay cognitive relay network with multiple PU transceivers. In this protocol, the secondary nodes can harvest energy from the primary network and share the licensed spectrum of it. In [24], a time division multiple access-based (TDMA-based) cooperative medium access control (MAC) protocol is proposed in CRNs with opportunistic energy harvesting. The licensed users lease a part of their spectrum to the unlicensed users to retransmit the failed packets on their behalf. In [25], the authors propose an efficient relay-based spectrum sharing protocol in CRNs, where the SU can implicitly harvest RF energy from the PU transmission. Both Alamouti coding and superposition coding techniques are adopted by the transmitters to facilitate primary data relaying and secondary data transmission simultaneously. The authors of [26] propose a novel information and energy cooperation strategy in a hierarchical CRN, where the PU is equipped with a time splitting energy harvesting device so that the primary system can share its spectrum to the secondary system and harvest energy from the secondary base station in return. In [27], the authors investigate beamforming for information and energy cooperation in cognitive non-regenerative two-way relay networks, and they consider a scenario that the ST knows imperfect CSI of all links. Similar to [27], the authors of [28] study a resource allocation problem of information and energy cooperation in two-way cognitive relay networks. In [29], the authors study an optimal design for a cooperation cognitive wireless-powered communication network with both amplify-and-forward (AF) and decode-and-forward (DF) relay protocols to maximize the energy efficiency of its uplink. The authors of [30] study a problem of information and energy cooperation in DF CRNs with full-duplex-enabled energy access points. In [31], the authors propose a novel cooperation model in CRNs, where one multi-antenna SU cooperates with two PUs to reach a three-party agreement on how to jointly share the licensed spectrum. Meanwhile, energy harvesting and spatial multiplexing are introduced to make full use of licensed spectrum and energy resources. In [32], the authors study the outage performance of a cooperative energy harvesting CRN, where the STs can harvest energy from the transmit signal of the PT and communicate with their respective receivers. Meanwhile, the STs will act as relays to assist the PT's transmission. However, in terms of information and energy cooperation

transmission, none of the related works mentioned above takes into account the physical layer security issue in cooperative CRNs.

The authors of [33]–[36] study the physical layer security issue either for SWIPT systems or cognitive two-way relay systems. However, they fail to integrate these three technologies of overlay spectrum sharing, RF energy harvesting, and physical layer security. In [37]–[44], the authors investigate a problem of physical layer security for information and energy cooperation transmission in cooperative CRNs. In [37], the AN-aided secrecy precoding problem of SWIPT is investigated for a cognitive multiple-input-multiple-output (MIMO) broadcast channel based on underlay spectrum sharing. In [38], the authors study a secure transmission scheme for dual-hop multi-antenna underlay spectrum sharing relaying systems. A maximum ratio combining/zero-forcing beamforming (MRC/ZFB) scheme at the relay is proposed to enhance secrecy performance. The authors of [39] study a robust AN-aided beamforming design problem for secure multiple-input-single-output (MISO) underlay CRNs based on a practical nonlinear energy harvesting model. In [40], the authors consider an underlay-based energy harvesting CRN and propose an energy-aware multiuser scheduling scheme, which takes into account both interference temperature constraint and residual energy level harvested from ambient surroundings. In [41], the authors consider a secure communication for an underlay cognitive untrusted relay network, and they examine connection outage probability and secrecy outage probability to investigate reliability and security performance in two cases, where the secondary destination exploits MRC or selection combining scheme. The authors of [42] consider cooperation between a primary system and a wireless-powered secondary system and study a secure information transmission problem for the primary system when the SUs are potential eavesdroppers. The authors of [43] study a problem of robust beamforming and power splitting for secure wireless information and power transfer in CRNs. Moreover, they consider that the ST knows imperfect CSI of a part link, and the PU may be malicious and might eavesdrop on the information signal intended for the SU. In [44], the authors study a secure beamforming design for an underlay- and overlay-based CRN. For both schemes, the SU is considered as a potential eavesdropper. However, the authors of [37]–[41] study the physical layer security issue in underlay-based cooperative CRNs, while the authors of [42]–[44] investigate the physical layer security issue in overlay-based cooperative CRNs with the consideration that the PU or SUs are just potential eavesdroppers rather than untrusted cooperative relays.

To the best of our knowledge, this work is the first to explore the problem of AN-aided secure wireless information and energy cooperation transmission in overlay spectrum sharing networks with untrusted cooperative dual-device-relay. A novel AN-aided joint time division- and power splitting-based three-phase secure wireless information and energy cooperation transmission strategy is proposed for overlay spectrum sharing networks, and we also investigate perfect and imperfect CSI on the impact of the system performance. For security consideration, we adopt the jamming signal to interference the unauthorized secondary system and set the confidential SINR constraints. It is worth noting that the secondary system is only allowed to use the AF relay protocol to help the primary system and prohibited it to use the DF relay protocol. Our purpose is to make the secondary system not know the signal to be relayed, but only to amplify and forward the relay signal and harvest energy from it (besides interfering with the untrusted relays to facilitate secure communication, the jamming signal is a new source for wireless power transfer as well and beneficial for harvesting energy). If the untrusted secondary system maliciously decodes the PU signal, it must satisfy the confidential SINR constraints. However, first of all, the untrusted secondary system has to satisfy the target data rate requirement of the primary system.

C. CONTRIBUTIONS

The main contributions of this paper are summarized as follows:

- We investigate a problem of security cooperation transmission between a single-antenna primary system and a multi-antenna wireless-powered untrusted secondary system, where the untrusted secondary devices can be regarded as potential malicious decoders. A novel AN-aided joint time division- and power splitting-based three-phase secure wireless information and energy cooperation transmission strategy is proposed for overlay spectrum sharing networks with untrusted cooperative dual-device-relay. Our proposal is a win-win and security-controllable cooperation strategy that integrates three technologies: Overlay spectrum sharing, RF energy harvesting, and physical layer security. Furthermore, to prevent the untrusted secondary devices from maliciously decoding the PT's signals, we adopt the source node-based AN-aided technique to protect the PU information and set the confidential SINR constraints. Besides, this paper not only considers the scenario of perfect CSI but also investigates imperfect CSI on the impact of the system performance.
- A new mathematical optimization problem is formulated to maximize the data rate of the untrusted secondary system, by jointly optimizing the time division ratios, the power splitting ratios, and the untrusted SUs' beamforming vectors and transmit power, subject to the PU's target data rate requirement and the untrusted SUs' energy harvesting constraints, power consumption constraints, and confidential SINR constraints. Through theoretical analysis and derivation, we equivalently transform the original optimization problem to obtain the untrusted SUs' optimal beamforming vectors and transmit power. Since the transformed optimization problem is still non-convex and improbable to be transformed into a convex problem, we will utilize the *fmincon Interior Point Algorithm* to solve and obtain

its locally optimal solution and corresponding function value. Additionally, we further analyze the complexity of the proposed optimization problem, and the optimization problem with imperfect CSI can also be solved by the same approach.

- Simulation results demonstrate that our proposed strategy is the best and significantly improves the average data rate of the untrusted secondary system under different PU target data rate requirements, PT rated transmit power, untrusted SU initial power, and PT power allocation ratios. We can draw the conclusions from simulation results that the more energy the untrusted secondary system harvests, the better performance it can achieve. Furthermore, the looser the confidential SINR constraints of the untrusted secondary system are, the better performance it can achieve, but the lower the confidentiality of the primary system will be. However, by adjusting the minimum durations, our proposed strategy not only significantly improves the average data rate of the untrusted secondary system, but also enables the primary system to achieve better confidentiality. Finally, a large number of simulations show that the time division ratios have a significant impact on the system performance, and these simulation results also verify the feasibility and effectiveness of the proposed strategy.

D. ORGANIZATION AND NOTATIONS

The rest of this paper is organized as follows. The system model is presented in section II. For perfect CSI, we formulate and solve the joint optimization problem of AN-aided time division- and power splitting-based three-phase secure wireless information and energy cooperation transmission in section III. The scenario of imperfect CSI can be found in section IV. Simulation results are presented in Section V. Finally, we conclude this paper in Section VI.

The following notations will be adopted in this paper. Vectors and matrices are represented by boldface lowercase and uppercase letters, respectively. $|\cdot|$ denotes the modulo operation. $\|\cdot\|$ denotes the Frobenius norm. $(\cdot)^\dagger$ denotes the Hermitian operation of a vector or matrix. $\mathbf{I}$ denotes an identity matrix of appropriate dimensions. $E[\cdot]$ denotes the expectation. $\mathcal{R}(\chi)$ denotes the real part of χ. $\mathbf{m} \sim \mathcal{CN}(\mathbf{0}, \mathbf{\Omega})$ denotes a vector $\mathbf{m}$ of complex Gaussian elements with a mean vector of $\mathbf{0}$ and a covariance matrix of $\mathbf{\Omega}$. $\mathbb{C}^{N\times 1}$ denotes the space of $N \times 1$ dimensional complex vector.

II. SYSTEM MODEL

We investigate the AN-aided secure wireless information and energy cooperation transmission in overlay spectrum sharing networks with untrusted cooperative dual-device-relay, as shown in Fig. 1. The primary system consists of a PT and a PU, while the untrusted secondary system consists of two secondary devices, where one secondary user (SU_1) serves the other secondary user (SU_2).[1] The primary system is equipped with a single antenna, and the untrusted secondary system is equipped with N antennas. The PT intends to transmit a confidential information s_p ($E[|s_p|^2] = 1$) to the PU, while the SU_1 sends a non-confidential information s_s ($E[|s_s|^2] = 1$) to the SU_2. We consider a scenario where the untrusted secondary system can share the licensed spectrum occupied by the primary system under the condition that these two SU_i, $i \in \{1, 2\}$, have to relay the PT's signals. However, when these two SU_i are low energy untrusted devices, security cooperation is difficult. Therefore, motivated by this, we propose an AN-aided joint time division- and power splitting-based three-phase secure wireless information and energy cooperation transmission strategy in overlay spectrum sharing networks with untrusted cooperative dual-device-relay. This scenario is typical for D2D communication in secure spectrum sharing networks, where one licensed user, such as a femtocell user, securely communicates with its base station with the help of two unlicensed untrusted energy-constrained mobile devices, while these two devices can communicate directly with each other under the condition that the licensed system provides spectrum and energy resources. Moreover, these unlicensed untrusted energy-constrained devices may also be wireless sensor devices, internet of things devices, or small-scale machine type communication devices.

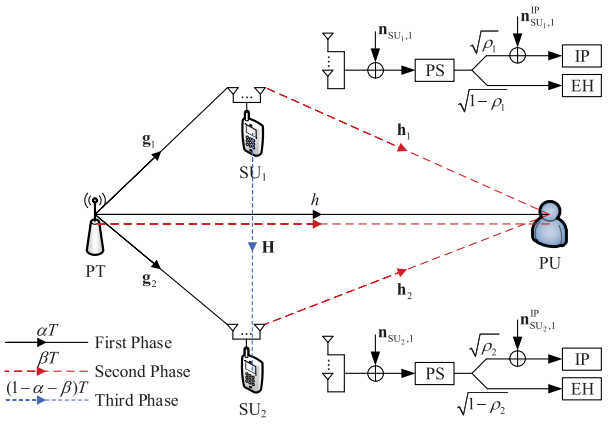

FIGURE 1. System model: An AN-aided joint time division- and power splitting-based three-phase secure wireless information and energy cooperation transmission model in overlay spectrum sharing networks with untrusted cooperative dual-device-relay.

During the first phase of length αT, the PT simultaneously transmits the confidential signal s_p and the jamming signal s_z ($E[|s_z|^2] = 1$), and then these two SU_i adopt the power splitting (PS) technique [45] to split the received signals from the PT into two separate signal streams with different power levels, one sent to the energy harvester (EH) and the other to the information processor (IP). During the second phase of

[1] In this untrusted secondary system, the SU_1 and the SU_2 can be exchanged with each other. In other words, the SU_1 can also be served by the SU_2.

length βT, these two SU_i utilize the beamforming technique to jointly forward the combined signals (the desired signal and the jamming signal) received from the first phase by using their initial power and harvested energy. We consider a situation where both SU_1 and SU_2 operate in half-duplex mode, so they cannot simultaneously transmit and receive signals in the same frequency. Therefore, the third phase of length $(1-\alpha-\beta)T$ is required to facilitate the direct communication between SU_1 and SU_2. Without loss of generality, we assume that the total communication duration T is normalized to unity.

To prevent the untrusted secondary devices from maliciously decoding the PT's signals, we adopt the source node-based AN-aided technique to protect the PU information and set the confidential SINR constraints. We assume that the artificial noise s_z transmitted by the PT can be removed at the PU, but cannot be eliminated at the two untrusted SU_i devices [46]–[48]. This method is based on channel independence and reciprocity [49], [50]. Specifically, the PU sends a pilot signal to the PT, and then the PT transmits a random key and modulates the phase of the transmitted signal with the received channel phase. Due to the randomness and independence of channels, the PU can decode the key while the channel phases between PT and SU_i are different from those between PT and PU. Hence, the key can be transmitted confidentially without being eavesdropped by other receivers [46]–[48]. Since the key is only known by the PT and the PU, they can use this key to generate a random complex Gaussian sequence by using a pseudo-random sequence generator [51].

Some common system parameters are introduced as follows. The channel coefficient of the PT-PU link is denoted by the complex scalar h. The $N\times 1$ dimensional complex channel vectors of the PT-SU_i and the SU_i-PU links are represented by $\mathbf{g}_i$ and $\mathbf{h}_i$, respectively. The $N\times N$ dimensional complex channel matrix of the SU_1-SU_2 link is represented by $\mathbf{H}$. The total energy (or average transmit power) of the PT is P_p, and the target data rate requirement of the PU is r_p. These two SU_i each have the initial total energy of P_{0,SU_i}, respectively, and they can further harvest energy from the PT. All channels and noise elements are assumed to be statistically independent of each other. Furthermore, these two SU_i are only allowed to use the AF relay protocol to jointly forwarding the combined signals received from the first phase.

We consider two types of noise on the terminal: One is received thermal noise, and the other is conversion noise from RF to baseband. These two types of noise are modeled as additive white Gaussian noise (AWGN) with a zero mean and the variances of N_0 and N_c, respectively. It is assumed that these two types of noise are independent of each other.

III. SECURE WIRELESS INFORMATION AND ENERGY COOPERATION TRANSMISSION WITH PERFECT CSI

In this section, we first detail the AN-aided joint time division- and power splitting-based three-phase secure wireless information and energy cooperation transmission strategy in overlay spectrum sharing networks with perfect CSI. Then, we formulate an optimization problem to maximize the data rate of the SU_2, subject to the PU's target data rate requirement and the SU_i's maximum power consumption constraints, maximum confidential SINR constraints, and minimum energy harvesting constraints, respectively. Finally, we present the solution and complexity analysis of the optimization problem. The scenario with imperfect CSI can be found in the next section.

A. PRIMARY USER SECURE WIRELESS INFORMATION TRANSMISSION AND SECONDARY USERS INFORMATION RECEIVING AND ENERGY HARVESTING IN THE FIRST PHASE

As shown in Fig. 1, the PT simultaneously transmits both the confidential signal s_p and the jamming signal s_z with the power levels λP_p and $(1-\lambda)P_p$, respectively. Thus, the transmit signal of the PT in the first two phases can be written as follows

$$t_{\mathrm{PT}} = \sqrt{\lambda P_p}s_p + \sqrt{(1-\lambda)P_p}s_z, \tag{1}$$

where λ is the power allocation ratio of the PT, $\lambda \in [0,1]$. With perfect CSI, since the jamming signal is known by the PU, it can completely cancel the jamming signal from the received combined signals. Thus, the received signal at the PU can be expressed as follows

$$y_{\mathrm{PU},1} = \sqrt{\lambda P_p}hs_p + n_{\mathrm{PU},1}, \tag{2}$$

where $n_{\mathrm{PU},1} \sim \mathcal{CN}(0, N_0)$ is the thermal noise received at the PU in the first phase. Hence, the achievable data rate of the PU can be expressed as follows

$$R_{\mathrm{PU},1} = \alpha \log_2\left(1+\frac{\lambda P_p|h|^2}{N_0}\right). \tag{3}$$

Since these two SU_i have no knowledge about the jamming signal s_z, the received signal at the SU_i can be expressed as follows

$$\begin{aligned}\mathbf{y}_{\mathrm{SU}_i,1} = {} & \sqrt{\lambda P_p}\mathbf{g}_i s_p + \sqrt{(1-\lambda)P_p}\mathbf{g}_i s_z \\ & + \mathbf{n}_{\mathrm{SU}_i,1}, \quad i\in\{1,2\},\end{aligned} \tag{4}$$

where $\mathbf{n}_{\mathrm{SU}_i,1} \sim \mathcal{CN}(\mathbf{0}, N_0\mathbf{I})$ are the thermal noises received at the SU_i, respectively.

After received the combined signals from the PT, these two SU_i split them into two parts: One is used to forward to the PU, and the other is used to harvest energy with the power splitting ratios of ρ_i and $1-\rho_i$, respectively. Thus, the signal for AF processing at the SU_i can be written as follows

$$\begin{aligned}\mathbf{y}^{\mathrm{IP}}_{\mathrm{SU}_i,1} &= \sqrt{\rho_i}\mathbf{y}_{\mathrm{SU}_i,1} + \mathbf{n}^{\mathrm{IP}}_{\mathrm{SU}_i,1} \\ &= \sqrt{\rho_i\lambda P_p}\mathbf{g}_i s_p + \sqrt{\rho_i(1-\lambda)P_p}\mathbf{g}_i s_z \\ &\quad + \sqrt{\rho_i}\mathbf{n}_{\mathrm{SU}_i,1} + \mathbf{n}^{\mathrm{IP}}_{\mathrm{SU}_i,1}, \quad i\in\{1,2\},\end{aligned} \tag{5}$$

where $\mathbf{n}^{\mathrm{IP}}_{\mathrm{SU}_i,1} \sim \mathcal{CN}(\mathbf{0}, N_c\mathbf{I})$ are complex AWGNs at the SU_i due to the conversion from the RF signal to the baseband signal.

For security consideration, if these two untrusted SU_i attempt to maliciously decode the information of the PU, they must satisfy the confidential SINR constraints as follows

$$SINR_{SU_i,1} = \frac{\rho_i \lambda \kappa_i}{\rho_i(1-\lambda)\kappa_i + \rho_i N_0 + N_c} \leq \gamma_i, \quad i \in \{1,2\}, \tag{6}$$

where κ_i can be defined as $\kappa_i \triangleq P_p \|\mathbf{g}_i\|^2$, and γ_i are the confidential SINR requirements of the PU.

The signal for harvesting energy at the SU_i can be written as follows

$$\begin{aligned} \mathbf{y}_{SU_i,1}^{EH} &= \sqrt{1-\rho_i}\mathbf{y}_{SU_i,1} \\ &= \sqrt{(1-\rho_i)\lambda P_p}\mathbf{g}_i s_p + \sqrt{(1-\rho_i)(1-\lambda)P_p}\mathbf{g}_i s_z \\ &\quad + \sqrt{1-\rho_i}\mathbf{n}_{SU_i,1}, \quad i \in \{1,2\}. \end{aligned} \tag{7}$$

Hence, the amount of the harvested energy at the SU_i can be expressed as follows

$$P_{SU_i,1}^{EH} = \alpha(1-\rho_i)\xi_i, \quad i \in \{1,2\}, \tag{8}$$

where ξ_i can be defined as $\xi_i \triangleq \eta_i(\kappa_i + N_0)$, and η_i denote the energy conversion efficiencies of the SU_i from signal power to circuit power.

B. PRIMARY USER WIRELESS INFORMATION TRANSMISSION AND FORWARDING IN THE SECOND PHASE

The information processing at the SU_i can be presented as $f(\mathbf{y}_{SU_i,1}) = \mathbf{A}_i \mathbf{y}_{SU_i,1}^{IP}$. Without loss of optimality, it has been proved in [52] that the optimal structure of $\mathbf{A}_i$ can be presented as $\mathbf{A}_i = \mathbf{w}_i \mathbf{g}_i^\dagger$, where $\mathbf{w}_i \in \mathbb{C}^{N\times 1}$ are the transmit beamforming vectors of the SU_i. Thus, the transmit signal of the SU_i can be expressed as follows

$$\begin{aligned} \mathbf{t}_{SU_i,2} &= \mathbf{w}_i \mathbf{g}_i^\dagger \mathbf{y}_{SU_i,1}^{IP} \\ &= \sqrt{\rho_i \lambda P_p}\mathbf{w}_i \|\mathbf{g}_i\|^2 s_p + \sqrt{\rho_i(1-\lambda)P_p}\mathbf{w}_i\|\mathbf{g}_i\|^2 s_z \\ &\quad + \sqrt{\rho_i}\mathbf{w}_i\mathbf{g}_i^\dagger \mathbf{n}_{SU_i,1} + \mathbf{w}_i \mathbf{g}_i^\dagger \mathbf{n}_{SU_i,1}^{IP}, \quad i \in \{1,2\}. \end{aligned} \tag{9}$$

Hence, the average transmit power of the SU_i can be expressed as follows

$$E[\|\mathbf{t}_{SU_i,2}\|^2] = (\rho_i \phi_i + \zeta_i)\|\mathbf{w}_i\|^2, \quad i \in \{1,2\}, \tag{10}$$

where ϕ_i and ζ_i can be defined as $\phi_i \triangleq (\kappa_i + N_0)\|\mathbf{g}_i\|^2$ and $\zeta_i \triangleq N_c\|\mathbf{g}_i\|^2$, respectively.

After removed the jamming signal s_z, the remaining received signal at the PU can be written as follows

$$\begin{aligned} y_{PU,2} &= \sqrt{\lambda P_p}(h + \sum_{i=1,2}\sqrt{\rho_i}\|\mathbf{g}_i\|^2 \mathbf{h}_i^\dagger \mathbf{w}_i)s_p \\ &\quad + \sum_{i=1,2}\mathbf{h}_i^\dagger \mathbf{w}_i(\sqrt{\rho_i}\mathbf{g}_i^\dagger \mathbf{n}_{SU_i,1} + \mathbf{g}_i^\dagger \mathbf{n}_{SU_i,1}^{IP}) + n_{PU,2}, \end{aligned} \tag{11}$$

where $n_{PU,2} \sim \mathcal{CN}(0, N_0)$ is the thermal noise received at the PU in the second phase. Thus, the achievable data rate of the PU can be expressed as follows

$$\begin{aligned} &R_{PU,2} \\ &= \beta \log_2\left(1 + \frac{\lambda P_p \left|h + \sum_{i=1,2}\sqrt{\rho_i}\|\mathbf{g}_i\|^2 \mathbf{h}_i^\dagger \mathbf{w}_i\right|^2}{\sum_{i=1,2}(\rho_i N_0 + N_c)|\mathbf{h}_i^\dagger \mathbf{w}_i|^2\|\mathbf{g}_i\|^2 + N_0}\right). \end{aligned} \tag{12}$$

To get a better reception gain, the PU will utilize the MRC as the best reception strategy. Thus, the sum data rate of the PU can be written as follows

$$R_{PU} = R_{PU,1} + R_{PU,2}. \tag{13}$$

C. SECONDARY USERS WIRELESS INFORMATION TRANSMISSION IN THE THIRD PHASE

In the third phase, the SU_1 transmits its own data signal s_s to the SU_2. Define $\mathbf{u} \in \mathbb{C}^{N\times 1}$ ($\|\mathbf{u}\|^2 = 1$) and q_s as the normalized beamforming vector and transmit power of the SU_1, respectively, which are used to send the SU's data signal. Hence, the transmit signal of the SU_1 can be expressed as follows

$$\mathbf{t}_{SU_1,3} = \sqrt{q_s}\mathbf{u}s_s. \tag{14}$$

After received the SU's data signal s_s, the SU_2 will use the normalized decoding vector $\mathbf{v} \in \mathbb{C}^{N\times 1}$ ($\|\mathbf{v}\|^2 = 1$) to decode the signal. Thus, the decoded signal of the SU_2 can be written as follows

$$y_{SU_2,3} = \sqrt{q_s}\mathbf{v}^\dagger \mathbf{H}\mathbf{u}s_s + \mathbf{v}^\dagger \mathbf{n}_{SU_2,3}, \tag{15}$$

where $\mathbf{n}_{SU_2,3} \sim \mathcal{CN}(\mathbf{0}, N_0\mathbf{I})$ is the thermal noise received at the SU_2 in the third phase. Therefore, the achievable data rate of the SU_2 can be expressed as follows

$$R_{SU_2,3} = (1-\alpha-\beta)\log_2\left(1 + \frac{q_s|\mathbf{v}^\dagger \mathbf{H}\mathbf{u}|^2}{N_0}\right). \tag{16}$$

To maximize the data rate of the SU_2, we can utilize the singular value decomposition (SVD) [53] of the channel gain matrix $\mathbf{H}$ to obtain the normalized beamforming vector $\mathbf{u}$ and the normalized decoding vector $\mathbf{v}$. Since both SU_1 and SU_2 are equipped with N antennas, the SVD of the channel gain matrix $\mathbf{H}$ can be presented as $\mathbf{H} = \mathbf{V}\mathbf{\Sigma}\mathbf{U}^\dagger$. $\mathbf{V}$ and $\mathbf{U}$ are the left singular vector matrix and the right singular vector matrix of $\mathbf{H}$, respectively. $\mathbf{\Sigma}$ is an N order diagonal matrix in which diagonal elements, $\sigma_1 \geq \sigma_2 \geq \cdots \geq \sigma_N \geq 0$, are the ordered singular values of matrix $\mathbf{H}$. When $\mathbf{v}$ equals the master left singular vector (the first column of $\mathbf{V}$), and $\mathbf{u}$ equals the master right singular vector (the first column of $\mathbf{U}$), the term $\mathbf{v}^\dagger\mathbf{H}\mathbf{u}$ will get its maximum value which equals the maximum singular value of matrix $\mathbf{H}$, i.e., $|\mathbf{v}^\dagger\mathbf{H}\mathbf{u}| = \sigma_1$.

D. OPTIMIZATION PROBLEM

In this subsection, we formulate an optimization problem with the objective to maximize the data rate of the SU_2, by jointly optimizing the time division ratios α and β,

the power splitting ratios ρ_1 and ρ_2, the transmit beamforming vectors $\mathbf{w}_1$ and $\mathbf{w}_2$, and the transmit power q_s, subject to the PU's target data rate requirement and the SU_i's maximum power consumption constraints, maximum confidential SINR constraints, and minimum energy harvesting constraints. Firstly, we define two minimum durations Δt_i, which are used to transmit and forward the PT's signals, respectively. These two minimum durations guarantee that the PT's signals can be received successfully in the first two phases. Secondly, we define two minimum power splitting ratios $\Delta\rho_i$, which ensure that the PT's signals can be successfully amplified and forwarded instead of being fully harvested as an energy signal. Finally, the optimization problem can be formulated as (17), as shown at the bottom of this page.

In the optimization problem (17), C1 denotes the target data rate requirement of the PU that the untrusted secondary system must satisfy first. C2 and C3 denote two maximum power consumption constraints of the SU_i, respectively. C4 denotes two maximum confidential SINR constraints for the SU_i. C5 denotes two minimum energy harvesting constraints of the SU_i, where Γ_1 and Γ_2 are the energy harvesting requirements of the SU_i, respectively. C6 denotes the definition domain of the variables. The limitations of α, β, ρ_i, r_p, γ_i, Γ_i are set to guarantee the security cooperation between the primary system and the untrusted secondary system. The energy conversion efficiencies η_i can be considered as a constant which are determined by the power transfer circuit.

E. THE SOLUTION OF THE OPTIMIZATION PROBLEM

In this subsection, we solve the optimization problem (17) through theoretical analysis and derivation. The optimization problem (17) is a non-convex problem and difficult to solve with seven variables (α, β, ρ_i, $\mathbf{w}_i$, q_s), simultaneously. First, for a given α, β, ρ_i, we equivalently transform the optimization problem (17) to obtain the optimal transmit beamforming vectors $\mathbf{w}_i^*$ and transmit power q_s^*. Then, after the equivalent transformation of the original problem, we will utilize the *fmincon* function to solve and obtain its locally optimal solution and the corresponding objective function value.

For a given α, β, ρ_i, the optimization problem (17) can be reformulated as follows

$$\begin{aligned}
&\max_{\mathbf{w}_i, q_s} \ q_s \\
&\text{s.t. C1: } \frac{\lambda P_p \left| h + \sum_{i=1,2} \sqrt{\rho_i} \|\mathbf{g}_i\|^2 \mathbf{h}_i^\dagger \mathbf{w}_i \right|^2}{\sum_{i=1,2} (\rho_i N_0 + N_c) |\mathbf{h}_i^\dagger \mathbf{w}_i|^2 \|\mathbf{g}_i\|^2 + N_0} \geq \gamma_p, \\
&\quad \text{C2: } \|\mathbf{w}_1\|^2 \leq \frac{P_{0,\mathrm{SU}_1} + \alpha(1-\rho_1)\xi_1 - (1-\alpha-\beta) q_s}{\beta(\rho_1 \phi_1 + \zeta_1)}, \\
&\quad \text{C3: } \|\mathbf{w}_2\|^2 \leq \frac{P_{0,\mathrm{SU}_2} + \alpha(1-\rho_2)\xi_2}{\beta(\rho_2 \phi_2 + \zeta_2)}, \\
&\quad \text{C4: } q_s \geq 0,
\end{aligned} \tag{18}$$

where γ_p can be defined as $\gamma_p \triangleq 2^{\frac{r_p - \alpha \log_2 \left(1 + \frac{\lambda P_p |h|^2}{N_0}\right)}{\beta}} - 1$.

According to (18), we can see that only the C2 constraint contains the objective function q_s. Therefore, the maximization problem of the objective function q_s can be regarded as the problem of maximizing the transmit power q_s in the C2 constraint. Furthermore, as the transmit power q_s increases, the square of the norm of the transmit beamforming vector of the SU_1, i.e., $\|\mathbf{w}_1\|^2$, decreases monotonically. Thus, to maximize the transmit power q_s, we can minimize the transmit beamforming vector $\|\mathbf{w}_1\|^2$ in the C2 constraint. Finally, the optimization problem (18) can be reformulated as follows

$$\begin{aligned}
&\min_{\mathbf{w}_i} \ \|\mathbf{w}_1\|^2 \\
&\text{s.t. C1: } \sum_{i=1,2} (\rho_i \lambda \kappa_i - \rho_i \gamma_p N_0 - \gamma_p N_c) \|\mathbf{g}_i\|^2 |\mathbf{h}_i^\dagger \mathbf{w}_i|^2 \\
&\qquad + 2\lambda\kappa_1 \Big[\sqrt{\rho_1} \mathcal{R}\big(h^\dagger (\mathbf{h}_1^\dagger \mathbf{w}_1)\big) \\
&\qquad + \sqrt{\rho_1 \rho_2} \|\mathbf{g}_2\|^2 \mathcal{R}\big(\mathbf{w}_1^\dagger \mathbf{h}_1 \mathbf{h}_2^\dagger \mathbf{w}_2\big) \Big] \\
&\qquad + 2\lambda\kappa_2 \sqrt{\rho_2} \mathcal{R}\big(h^\dagger (\mathbf{h}_2^\dagger \mathbf{w}_2)\big) + \lambda P_p |h|^2 - \gamma_p N_0 \geq 0, \\
&\quad \text{C2: } \|\mathbf{w}_2\|^2 \leq \frac{P_{0,\mathrm{SU}_2} + \alpha(1-\rho_2)\xi_2}{\beta(\rho_2 \phi_2 + \zeta_2)}.
\end{aligned} \tag{19}$$

It is easy to see from the optimization problem (19) that the optimal transmit beamforming vectors $\mathbf{w}_i$ admit the form $\mathbf{w}_i^* = \sqrt{q_i} \frac{\mathbf{h}_i}{\|\mathbf{h}_i\|}$, where q_1 and q_2 are the transmit

$$\begin{aligned}
&\max_{\alpha, \beta, \rho_i, \mathbf{w}_i, q_s} \ (1-\alpha-\beta) \log_2 \left(1 + \frac{q_s \sigma_1^2}{N_0}\right) \\
&\text{s.t. C1: } \alpha \log_2 \left(1 + \frac{\lambda P_p |h|^2}{N_0}\right) + \beta \log_2 \left(1 + \frac{\lambda P_p \left| h + \sum_{i=1,2} \sqrt{\rho_i} \|\mathbf{g}_i\|^2 \mathbf{h}_i^\dagger \mathbf{w}_i \right|^2}{\sum_{i=1,2} (\rho_i N_0 + N_c) |\mathbf{h}_i^\dagger \mathbf{w}_i|^2 \|\mathbf{g}_i\|^2 + N_0}\right) \geq r_p, \\
&\quad \text{C2: } \beta(\rho_1 \phi_1 + \zeta_1) \|\mathbf{w}_1\|^2 + (1-\alpha-\beta) q_s \leq P_{0,\mathrm{SU}_1} + \alpha(1-\rho_1)\xi_1, \\
&\quad \text{C3: } \beta(\rho_2 \phi_2 + \zeta_2) \|\mathbf{w}_2\|^2 \leq P_{0,\mathrm{SU}_2} + \alpha(1-\rho_2)\xi_2, \\
&\quad \text{C4: } \frac{\rho_i \lambda \kappa_i}{\rho_i (1-\lambda)\kappa_i + \rho_i N_0 + N_c} \leq \gamma_i, \quad i \in \{1, 2\}, \\
&\quad \text{C5: } \alpha(1-\rho_i)\xi_i \geq \Gamma_i, \quad i \in \{1, 2\}, \\
&\quad \text{C6: } \alpha + \beta \leq 1, \ q_s \geq 0, \ \Delta t_1 \leq \alpha \leq 1 - \Delta t_2, \ \Delta t_2 \leq \beta \leq 1 - \Delta t_1, \ \Delta\rho_i \leq \rho_i \leq 1, \ i \in \{1, 2\},
\end{aligned} \tag{17}$$

power of the SU_i, respectively, and they can be defined as $q_i \triangleq \|\mathbf{w}_i\|^2$. Substituting $\mathbf{w}_i^*$ into the optimization problem (19), then we can obtain the optimization problem (20) as follows

$$\begin{aligned}
&\min_{q_1,q_2} \ q_1 \\
&\text{s.t. C1: } (\rho_1\lambda\kappa_1 - \rho_1\gamma_p N_0 - \gamma_p N_c)\|\mathbf{g}_1\|^2\|\mathbf{h}_1\|^2(\sqrt{q_1})^2 \\
&\quad + 2\lambda\kappa_1\|\mathbf{h}_1\|\left(\mathcal{R}(h)\sqrt{\rho_1}+\|\mathbf{g}_2\|^2\|\mathbf{h}_2\|\sqrt{\rho_1\rho_2 q_2}\right)\sqrt{q_1} \\
&\quad + (\rho_2\lambda\kappa_2 - \rho_2\gamma_p N_0 - \gamma_p N_c)\|\mathbf{g}_2\|^2\|\mathbf{h}_2\|^2 q_2 \\
&\quad + 2\lambda\kappa_2\|\mathbf{h}_2\|\mathcal{R}(h)\sqrt{\rho_2 q_2} + \lambda P_p|h|^2 - \gamma_p N_0 \geq 0, \\
&\text{C2: } q_2 \leq \frac{P_{0,\mathrm{SU}_2} + \alpha(1-\rho_2)\xi_2}{\beta(\rho_2\phi_2+\zeta_2)}, \\
&\text{C3: } q_1 \geq 0,\ q_2 \geq 0.
\end{aligned} \tag{20}$$

Theorem 1: The optimal transmit power of the SU_1 can be expressed as follows

$$q_s^* = \frac{P_{0,\mathrm{SU}_1} + \alpha(1-\rho_1)\xi_1 - \beta(\rho_1\phi_1+\zeta_1)q_1^*}{1-\alpha-\beta}. \tag{21}$$

Proof: Please refer to Appendix A. ■

According to Theorem 1, the optimization problem (17) can be equivalently transformed as follows

$$\begin{aligned}
&\max_{\alpha,\beta,\rho_i} \ (1-\alpha-\beta)\log_2\left(1+\frac{q_s^*\sigma_1^2}{N_0}\right) \\
&\text{s.t. C1: } \frac{\rho_i\lambda\kappa_i}{\rho_i(1-\lambda)\kappa_i + \rho_i N_0 + N_c} \leq \gamma_i, \quad i \in \{1,2\}, \\
&\quad \text{C2: } \alpha(1-\rho_i) \geq \frac{\Gamma_i}{\xi_i}, \quad i \in \{1,2\}, \\
&\quad \text{C3: } \alpha+\beta \leq 1,\ \Delta\rho_i \leq \rho_i \leq 1,\ i \in \{1,2\}, \\
&\qquad \Delta t_1 \leq \alpha \leq 1-\Delta t_2,\ \Delta t_2 \leq \beta \leq 1-\Delta t_1.
\end{aligned} \tag{22}$$

We can observe that the optimization problem (22) is still non-convex due to the high-order product form of variables contained in the objective function q_s^* and improbable to be transformed into a convex problem. To solve this nonlinearly constrained optimization problem, we will utilize the *fmincon* function in *MATLAB* (invoking the interior point algorithm) to solve and obtain its locally optimal solution and the corresponding objective function value, where the starting point can be set to (0.45,0.45,0.5,0.5). Furthermore, the solution to the optimization problem (22) is also the solution to the optimization problem (17) due to the equivalent transformation between them.

F. COMPLEXITY ANALYSIS

In this subsection, we present the complexity analysis of the optimization problem (22), and different from other sections, the symbols used in this subsection are gradually given below. As mentioned above, we utilize the *fmincon* function to solve the nonlinearly constrained optimization problem (22). Next, we briefly introduce the *fmincon Interior Point Algorithm* [54], [55]. Generally, a nonlinearly constrained optimization problem has the form as follows

$$\begin{aligned}
&\min_x f(x) \\
&\text{s.t. } h(x) = 0, \\
&\quad g(x) \leq 0,
\end{aligned}$$

where $f : \mathbb{R}^n \to \mathbb{R}$, $h : \mathbb{R}^n \to \mathbb{R}^k$ and $g : \mathbb{R}^n \to \mathbb{R}^m$ are twice continuously differentiable functions. The interior point method for constrained minimization is to solve a sequence of approximate minimization problems, i.e., a sequence of barrier subproblems. Therefore, the approximate problem can be expressed as follows

$$\begin{aligned}
&\min_{x,s} f_\mu(x,s) = f(x) - \mu\sum_{j=1}^{m}\ln s_j \\
&\text{s.t. } h(x) = 0, \\
&\quad g(x) + s = 0,
\end{aligned}$$

where $s > 0$ is a vector of slack variables, and $\mu > 0$ is the barrier parameter. As μ decreases to zero, the minimum of f_μ should approach the minimum of f. The Lagrangian function for this approximate problem can be expressed as follows

$$\mathcal{L}(x,s,\lambda_h,\lambda_g,\mu) = f_\mu(x,s) + \lambda_h^T h(x) + \lambda_g^T\big(g(x)+s\big),$$

where $\lambda_h \in \mathbb{R}^k$ and $\lambda_g \in \mathbb{R}^m$ are Lagrange multipliers.

It is pointed out in [54] that in order to solve this approximate problem, the algorithm uses one of two main types of steps at each iteration:

- A *Direct* step in $z = (x, s)$. This step attempts to solve the KKT equations for the approximate problem by a linear approximation. This is also called a *Newton* step.
- A *Conjugate Gradient (CG)* step using a trust region.

By default, the algorithm first tries to take a direct step. If cannot, it attempts a CG step. There is a case where it does not take a direct step when the approximate problem is not locally convex near the current iterate.

For the Newton method, the number of iterations required to produce a solution within an accuracy ϵ is no more than

$$L_1 = \frac{20-8\alpha}{\alpha\beta(1-2\alpha)^2}\big(f(z^{(0)}) - f(z^\star)\big) + \log_2\log_2(1/\epsilon),$$

where α and β are the backtracking line search parameters, and $z^{(0)}$ and $z^\star$ denote the starting point and the optimal point, respectively [56]. If the projected Hessian that obtained from the direct step is not positive definite, the algorithm uses the CG step.

The CG method is to minimize a quadratic approximation for the approximate problem in a trust region, subject to linearized constraints [54]. It is pointed out in [56] that the steepest descent method for an arbitrary norm is linear convergence, which is the same as the gradient method with backtracking line search (the number of iterations of the CG method is no more than that of the gradient method).

In particular, it will converge after at most

$$L_2 = \frac{\log\left((f(z^{(0)}) - f(z^{\star}))/\epsilon\right)}{\log(1/c)},$$

iterations of the gradient method with backtracking line search, where $c = 1 - \min\{2m\alpha, 2\beta\alpha m/M\} < 1$, and M/m is an upper bound on the condition number.

For the barrier method, the number of outer steps required within the desired accuracy ϵ is no more than

$$B = \left\lceil \frac{\log\left(m/(t^{(0)}\epsilon)\right)}{\log \mu} \right\rceil,$$

where $m/t^{(0)}$ is the duality gap that results from the first centering step [56].

Furthermore, the computational complexity of the Newton method and the gradient method are $\mathcal{O}(n^3)$ and $\mathcal{O}(n)$, respectively. Therefore, the sum computational complexity of the optimization problem (22) is no more than $\mathcal{O}\big(B(n^3L_1 + nL_2)\big)$.

IV. SECURE WIRELESS INFORMATION AND ENERGY COOPERATION TRANSMISSION WITH IMPERFECT CSI

In the previous section, we consider that the channel state information of all links is perfect. In this section, we assume that these two SU_i may obtain the perfect CSIs of $\mathbf{g}_i$ through channel estimation, and get the imperfect CSIs of $\mathbf{h}_i$ by utilizing the channel reciprocity in time division duplex systems. Due to the duplex delay between uplink and downlink, there is a certain degree of mismatch between the estimated CSIs ($\hat{\mathbf{h}}_i$) and the real CSIs ($\mathbf{h}_i$). Therefore, the relationship between the real $\mathbf{h}_i$ and the estimated $\hat{\mathbf{h}}_i$ can be expressed as follows

$$\mathbf{h}_i = \sqrt{\epsilon_i}\hat{\mathbf{h}}_i + \sqrt{1-\epsilon_i}\mathbf{e}_i, \quad i \in \{1, 2\}, \tag{23}$$

where $\mathbf{e}_i$ denote the estimation error vectors, which are independent and identically distributed (i.i.d.) complex Gaussian random variables with $\mathbf{e}_i \sim \mathcal{CN}(\mathbf{0}, \mathbf{I})$. ϵ_i denote the correlation coefficients between $\mathbf{h}_i$ and $\hat{\mathbf{h}}_i$, $\epsilon_i \in [0, 1]$. The larger the correlation coefficient is, the more accurate the channel estimation will be. If $\epsilon_i = 1$, these two SU_i will have the perfect CSIs about $\mathbf{h}_i$.

According to (11), in the scenario of imperfect CSI, the real jamming signal $\sum_{i=1,2}\sqrt{\rho_i(1-\lambda)P_p}\|\mathbf{g}_i\|^2\mathbf{h}_i^{\dagger}\mathbf{w}_i s_z$ in the received signals cannot be eliminated perfectly, while the estimated jamming signal $\sum_{i=1,2}\sqrt{\rho_i(1-\lambda)P_p\epsilon_i}\|\mathbf{g}_i\|^2\hat{\mathbf{h}}_i^{\dagger}\mathbf{w}_i s_z$ can be removed entirely. Therefore, after removed the estimated jamming signal, the remaining received signal of the PU in the second phase can be expressed as follows

$$\begin{aligned}
&\hat{y}_{\mathrm{PU},2} \\
&= \sqrt{\lambda P_p}\Big[h + \sum_{i=1,2}\sqrt{\rho_i}\|\mathbf{g}_i\|^2(\sqrt{\epsilon_i}\hat{\mathbf{h}}_i + \sqrt{1-\epsilon_i}\mathbf{e}_i)^{\dagger}\mathbf{w}_i\Big]s_p \\
&\quad + n_{\mathrm{PU},2} + \sum_{i=1,2}\sqrt{\rho_i(1-\lambda)P_p(1-\epsilon_i)}\|\mathbf{g}_i\|^2\mathbf{e}_i^{\dagger}\mathbf{w}_i s_z \\
&\quad + \sum_{i=1,2}(\sqrt{\epsilon_i}\hat{\mathbf{h}}_i + \sqrt{1-\epsilon_i}\mathbf{e}_i)^{\dagger}\mathbf{w}_i(\sqrt{\rho_i}\mathbf{g}_i^{\dagger}\mathbf{n}_{\mathrm{SU}_i,1} + \mathbf{g}_i^{\dagger}\mathbf{n}^{\mathrm{IP}}_{\mathrm{SU}_i,1}).
\end{aligned} \tag{24}$$

Thus, with imperfect CSI, the achievable data rate of the PU in the second phase can be written as (25), as shown at the bottom of this page.

Substituting (25) into the second term of the C1 constraint of the optimization problem (17), then we can obtain a new optimization problem with imperfect CSI. Similar to solve the optimization problem (17), this new optimization problem with imperfect CSI can be reformulated as (26), as shown at the bottom of this page, where ϑ_i can be defined as $\vartheta_i \triangleq \kappa_i(1-\lambda) + N_0$.

$$\hat{R}_{\mathrm{PU},2} = \beta\log_2\left(1 + \frac{\lambda P_p\left|h + \sum_{i=1,2}\sqrt{\rho_i}\|\mathbf{g}_i\|^2(\sqrt{\epsilon_i}\hat{\mathbf{h}}_i + \sqrt{1-\epsilon_i}\mathbf{e}_i)^{\dagger}\mathbf{w}_i\right|^2}{\sum_{i=1,2}\left[\rho_i\kappa_i(1-\lambda)(1-\epsilon_i)|\mathbf{e}_i^{\dagger}\mathbf{w}_i|^2 + (\rho_i N_0 + N_c)\left|(\sqrt{\epsilon_i}\hat{\mathbf{h}}_i + \sqrt{1-\epsilon_i}\mathbf{e}_i)^{\dagger}\mathbf{w}_i\right|^2\right]\|\mathbf{g}_i\|^2 + N_0}\right). \tag{25}$$

$$\begin{aligned}
&\min_{\mathbf{w}_i} \ \|\mathbf{w}_1\|^2 \\
&\text{s.t. C1: } \sum_{i=1,2}\Big[(\rho_i\lambda\kappa_i - \rho_i\gamma_p N_0 - \gamma_p N_c)\big(\epsilon_i|\hat{\mathbf{h}}_i^{\dagger}\mathbf{w}_i|^2 + 2\sqrt{\epsilon_i(1-\epsilon_i)}\mathcal{R}(\mathbf{w}_i^{\dagger}\hat{\mathbf{h}}_i\mathbf{e}_i^{\dagger}\mathbf{w}_i)\big) \\
&\quad + (\rho_i\lambda\kappa_i - \rho_i\gamma_p\vartheta_i - \gamma_p N_c)(1-\epsilon_i)|\mathbf{e}_i^{\dagger}\mathbf{w}_i|^2\Big]\|\mathbf{g}_i\|^2 \\
&\quad + \sum_{i=1,2}2\lambda\kappa_i\sqrt{\rho_i}\Big[\sqrt{\epsilon_i}\mathcal{R}\big(h^{\dagger}(\hat{\mathbf{h}}_i^{\dagger}\mathbf{w}_i)\big) + \sqrt{1-\epsilon_i}\mathcal{R}\big(h^{\dagger}(\mathbf{e}_i^{\dagger}\mathbf{w}_i)\big)\Big] \\
&\quad + 2\lambda\kappa_1\|\mathbf{g}_2\|^2\sqrt{\rho_1\rho_2}\Big[\sqrt{\epsilon_1\epsilon_2}\mathcal{R}(\mathbf{w}_1^{\dagger}\hat{\mathbf{h}}_1\hat{\mathbf{h}}_2^{\dagger}\mathbf{w}_2) + \sqrt{\epsilon_1(1-\epsilon_2)}\mathcal{R}(\mathbf{w}_1^{\dagger}\hat{\mathbf{h}}_1\mathbf{e}_2^{\dagger}\mathbf{w}_2) \\
&\quad + \sqrt{(1-\epsilon_1)\epsilon_2}\mathcal{R}(\mathbf{w}_1^{\dagger}\mathbf{e}_1\hat{\mathbf{h}}_2^{\dagger}\mathbf{w}_2) + \sqrt{(1-\epsilon_1)(1-\epsilon_2)}\mathcal{R}(\mathbf{w}_1^{\dagger}\mathbf{e}_1\mathbf{e}_2^{\dagger}\mathbf{w}_2)\Big] + \lambda P_p|h|^2 - \gamma_p N_0 \geq 0, \\
&\text{C2: } \|\mathbf{w}_2\|^2 \leq \frac{P_{0,\mathrm{SU}_2} + \alpha(1-\rho_2)\xi_2}{\beta(\rho_2\phi_2 + \zeta_2)},
\end{aligned} \tag{26}$$

$$
\begin{aligned}
&\min_{\hat{q}_1\geq 0,\hat{q}_2\geq 0} \quad \hat{q}_1 \\
&\text{s.t.} \quad \text{C1:} \Big\{(\rho_1\lambda\kappa_1-\rho_1\gamma_p N_0-\gamma_p N_c)\Big[\epsilon_1\|\hat{\mathbf{h}}_1\|^2+2\sqrt{\epsilon_1(1-\epsilon_1)}\mathcal{R}(\mathbf{e}_1^{\dagger}\hat{\mathbf{h}}_1)\Big] \\
&\quad + (\rho_1\lambda\kappa_1-\rho_1\gamma_p\vartheta_1-\gamma_p N_c)(1-\epsilon_1)\frac{|\mathbf{e}_1^{\dagger}\hat{\mathbf{h}}_1|^2}{\|\hat{\mathbf{h}}_1\|^2}\Big\}\|\mathbf{g}_1\|^2(\sqrt{\hat{q}_1})^2 \\
&\quad + \Big\{2\lambda\kappa_1\sqrt{\rho_1}\Big[\sqrt{\epsilon_1}\|\hat{\mathbf{h}}_1\|\mathcal{R}(h)+\frac{\sqrt{1-\epsilon_1}}{\|\hat{\mathbf{h}}_1\|}\mathcal{R}\big(h^{\dagger}(\mathbf{e}_1^{\dagger}\hat{\mathbf{h}}_1)\big)\Big] \\
&\quad + 2\lambda\kappa_1\|\mathbf{g}_2\|^2\sqrt{\rho_1\rho_2\hat{q}_2}\Big[\sqrt{\epsilon_1\epsilon_2}\|\hat{\mathbf{h}}_1\|\|\hat{\mathbf{h}}_2\|+\sqrt{\epsilon_1(1-\epsilon_2)}\frac{\|\hat{\mathbf{h}}_1\|}{\|\hat{\mathbf{h}}_2\|}\mathcal{R}(\mathbf{e}_2^{\dagger}\hat{\mathbf{h}}_2) \\
&\quad + \sqrt{(1-\epsilon_1)\epsilon_2}\frac{\|\hat{\mathbf{h}}_2\|}{\|\hat{\mathbf{h}}_1\|}\mathcal{R}(\hat{\mathbf{h}}_1^{\dagger}\mathbf{e}_1)+\frac{\sqrt{(1-\epsilon_1)(1-\epsilon_2)}}{\|\hat{\mathbf{h}}_1\|\|\hat{\mathbf{h}}_2\|}\mathcal{R}(\hat{\mathbf{h}}_1^{\dagger}\mathbf{e}_1\mathbf{e}_2^{\dagger}\hat{\mathbf{h}}_2)\Big]\Big\}\sqrt{\hat{q}_1} \\
&\quad + \Big\{(\rho_2\lambda\kappa_2-\rho_2\gamma_p N_0-\gamma_p N_c)\Big[\epsilon_2\|\hat{\mathbf{h}}_2\|^2+2\sqrt{\epsilon_2(1-\epsilon_2)}\mathcal{R}(\mathbf{e}_2^{\dagger}\hat{\mathbf{h}}_2)\Big] \\
&\quad + (\rho_2\lambda\kappa_2-\rho_2\gamma_p\vartheta_2-\gamma_p N_c)(1-\epsilon_2)\frac{|\mathbf{e}_2^{\dagger}\hat{\mathbf{h}}_2|^2}{\|\hat{\mathbf{h}}_2\|^2}\Big\}\|\mathbf{g}_2\|^2\hat{q}_2 \\
&\quad + 2\lambda\kappa_2\sqrt{\rho_2}\Big[\sqrt{\epsilon_2}\|\hat{\mathbf{h}}_2\|\mathcal{R}(h)+\frac{\sqrt{1-\epsilon_2}}{\|\hat{\mathbf{h}}_2\|}\mathcal{R}\big(h^{\dagger}(\mathbf{e}_2^{\dagger}\hat{\mathbf{h}}_2)\big)\Big]\sqrt{\hat{q}_2}+\lambda P_p|h|^2-\gamma_p N_0\geq 0, \\
&\text{C2:} \ \hat{q}_2\leq\frac{P_{0,\mathrm{SU}_2}+\alpha(1-\rho_2)\xi_2}{\beta(\rho_2\phi_2+\zeta_2)}.
\end{aligned}
\tag{27}
$$

From the optimization problem (26) we can see that the optimal transmit beamforming vectors $\hat{\mathbf{w}}_i$ for imperfect CSI admit the form $\hat{\mathbf{w}}_i^*=\sqrt{\hat{q}_i}\frac{\hat{\mathbf{h}}_i}{\|\hat{\mathbf{h}}_i\|}$, where $\hat{q}_1$ and $\hat{q}_2$ are the transmit power of the SU_i for imperfect CSI, respectively. Substituting $\hat{\mathbf{w}}_i^*$ into the optimization problem (26), then we can obtain the optimization problem (27), as shown at the top of this page.

Theorem 2: The optimal transmit power of the SU_1 in the presence of imperfect CSI can be expressed as follows

$$
\hat{q}_s^*=\frac{P_{0,\mathrm{SU}_1}+\alpha(1-\rho_1)\xi_1-\beta(\rho_1\phi_1+\zeta_1)\hat{q}_1^*}{1-\alpha-\beta}. \tag{28}
$$

Proof: Please refer to Appendix B. ■

According to Theorem 2, we replace the q_s^* of the optimization problem (22) with the $\hat{q}_s^*$, and then we can obtain an optimization problem with imperfect CSI, which similar to the optimization problem (22). Since the structure of this optimization problem with imperfect CSI is similar to that of the optimization problem (22), we can still use the *fmincon Interior Point Algorithm* to solve and obtain its locally optimal solution and the corresponding objective function value as mentioned in section III F.

Moreover, the computational complexity of this optimization problem with imperfect CSI is the same as the optimization problem (22) due to the same structure between them.

V. SIMULATION RESULTS

In this section, the performance results of the proposed strategy are presented by simulation studies. If not specified, simulation settings are given as follows. Both SU_1 and SU_2 are equipped with $N=4$ antennas. The distances between PT and PU, PT and SU_i, SU_i and PU, SU_1 and SU_2 are set to $\sqrt{3}$ m, 1 m, 1 m, 1 m, respectively. The channel between a transmit-receive antenna pair is modeled as $h=(d)^{-\frac{l}{2}}e^{j\omega}$ [15], where d is the distance, l is the path loss exponent, chosen as 3.5, and ω is uniformly distributed over $[0,2\pi)$. The variances of the noise are normalized to unity, i.e., $N_0=N_C=1$. The transmit power of the PT is $P_p=33$ dBm. The target rate requirement of the PU is $r_p=3$ bps/Hz. The power allocation ratio of the PT is $\lambda=0.5$. The correlation coefficients between $\mathbf{h}_i$ and $\hat{\mathbf{h}}_i$ are $\epsilon_1=\epsilon_2=0.9$. The initial power of the SU_i are $P_{0,\mathrm{SU}_1}=P_{0,\mathrm{SU}_2}=0$ dBm. The two minimum durations and two minimum power splitting ratios are $\Delta t_1=\Delta t_2=0.2$ and $\Delta\rho_1=\Delta\rho_2=0.1$, respectively. All simulation results are averaged over 10000 channel realizations. Furthermore, our proposed strategy needs to follow the access principle of overlay spectrum sharing networks as detailed below. If the direct link of the primary system can support the target rate requirement of the PU, the PU does not need relay assistance, i.e., if $R_{\mathrm{PU},1}\geq r_p$, then $R_{\mathrm{SU}_2,3}=0$. Besides, if the two secondary devices act as pure untrusted relays still cannot satisfy the target rate requirement of the PU, the whole system outage occurs, i.e., if $R_{\mathrm{PU}}<r_p$, then $R_{\mathrm{SU}_2,3}=0$.

To compare the performance of different schemes, we propose three heuristic schemes. **Heuristic Scheme 1**: Adjust the two power splitting ratios to make them equal to ρ, i.e., $\rho_1=\rho_2=\rho$. In this way, the number of variables

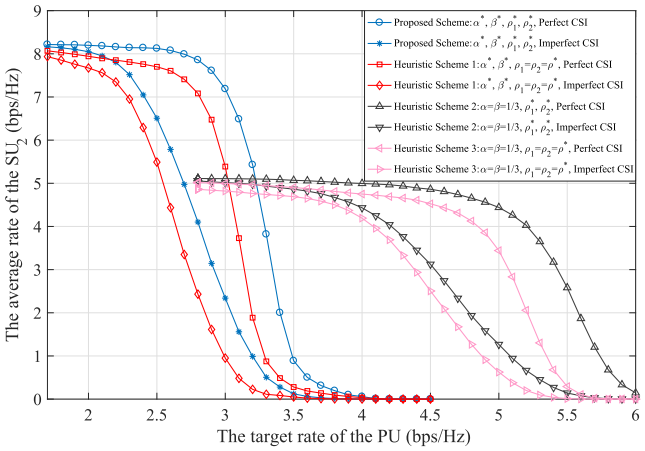

FIGURE 2. The target rate of the PU vs the average rate of the SU_2: Comparison of different schemes with perfect and imperfect CSI for $\Gamma_1 = \Gamma_2 = 10$ dBm, $\gamma_1 = \gamma_2 = 0$ dB, $\eta_1 = \eta_2 = 0.6$.

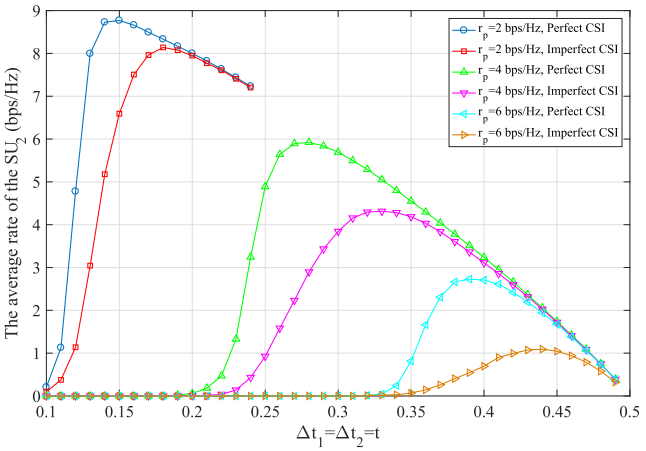

FIGURE 3. The minimum durations of the first two phases vs the average rate of the SU_2: Comparison of different PU target rate requirements with perfect and imperfect CSI for $\Gamma_1 = \Gamma_2 = 10$ dBm, $\gamma_1 = \gamma_2 = 0$ dB, $\eta_1 = \eta_2 = 0.6$.

can be reduced from four to three, i.e., (α, β, ρ). **Heuristic Scheme 2**: Adjust the two time division ratios to make them equal to 1/3, i.e., $\alpha = \beta = 1/3$. In this way, the number of variables can be reduced from four to two, i.e., $(1/3, 1/3, \rho_1, \rho_2)$. **Heuristic Scheme 3**: Adjust the two time division ratios and two power splitting ratios to make them equal to 1/3 and ρ, respectively. In this way, the number of variables can be reduced from four to one, i.e., $(1/3, 1/3, \rho)$.

The performance results of different schemes with perfect and imperfect CSI under varying PU target rate requirements are compared in Fig. 2. From Fig. 2, we can see that the average rate of the SU_2 of the proposed scheme and heuristic scheme 1 outperforms that of the heuristic scheme 2 and 3 in the low PU target rate region. However, the average rate of the SU_2 of the heuristic scheme 2 and 3 is superior to that of the other two schemes in the medium to high PU target rate region. Since the proposed scheme aims to maximize the data rate of the untrusted secondary system, these two time division ratios tend to be minimal, and thus the PU target rate that the untrusted secondary system can support is low. However, the heuristic scheme 2 and 3 can support a higher PU target rate than the other two schemes due to the larger minimum durations. If the minimum durations continue to increase and exceed 1/3, the PU target rate will also increase, while the average rate of the SU_2 will decrease. Furthermore, we can also observe that the average rate of the SU_2 of the proposed scheme is superior to that of the heuristic scheme 1, and the average rate of the SU_2 of the heuristic scheme 2 outperforms that of the heuristic scheme 3.

Fig. 3 shows the impact of the minimum durations on the average rate of the SU_2 with perfect and imperfect CSI under different PU target rate requirements. As can be seen from Fig. 3, when a PU target rate is given, an optimal minimum duration can be determined, which corresponds to the maximum average rate of the SU_2. When the PU target rate requirement is equal to 6 bps/Hz, the maximum average rates of the SU_2 with perfect and imperfect CSI are equal to 2.73 bps/Hz and 1.09 bps/Hz, respectively, which are obviously larger than the average rates corresponding to the heuristic scheme 2 in Fig. 2. Therefore, the proposed scheme is the best by adjusting the minimum durations under different PU target rate requirements.

The performance results of different minimum energy harvesting requirements with perfect and imperfect CSI under varying PU target rate requirements are compared in Fig. 4. We can observe from Fig. 4 that the average rate of the SU_2 with the minimum energy harvesting requirements $\Gamma_1 = \Gamma_2 = 17$ dBm is superior to that with $\Gamma_1 = \Gamma_2 = 10$ dBm. However, the performance gap between different minimum energy harvesting requirements with perfect CSI is very small, while the performance gap with imperfect CSI is relatively large. Due to the impact of imperfect CSI, the untrusted secondary system will consume more energy to help the PU satisfy its target rate requirement. For imperfect CSI, the residual energy of the untrusted secondary system with $\Gamma_1 = \Gamma_2 = 10$ dBm is less than that with $\Gamma_1 = \Gamma_2 = 17$ dBm, so the performance gap between them is more clearly. We can draw a conclusion that the more energy the untrusted secondary system harvests, the better performance it can achieve. In Fig. 4, we can also see that there is a clear performance gap between perfect and imperfect CSI, and the performance of perfect CSI is always better than that of imperfect CSI. Besides, the performance of the energy conversion efficiencies with $\eta_1 = \eta_2 = 0.6$ is always better than that with $\eta_1 = \eta_2 = 0.3$.

Fig. 5 shows the performance comparison between different maximum confidential SINR requirements with perfect and imperfect CSI under varying PU target rate requirements. As shown in Fig. 5, the average rate of the SU_2 with the maximum confidential SINR requirements $\gamma_1 = \gamma_2 = 10$ dB is better than that with $\gamma_1 = \gamma_2 = 0$ dB. However, the performance gap between different maximum confidential SINR

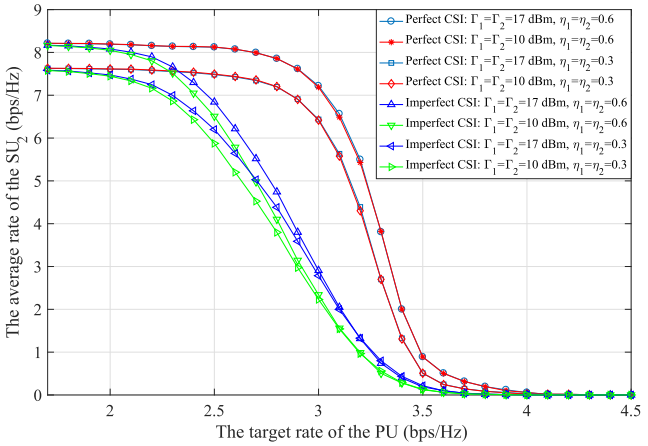

FIGURE 4. The target rate of the PU vs the average rate of the SU_2 with varying energy conversion efficiencies: Comparison between different minimum energy harvesting requirements with perfect and imperfect CSI for $\gamma_1 = \gamma_2 = 0$ dB.

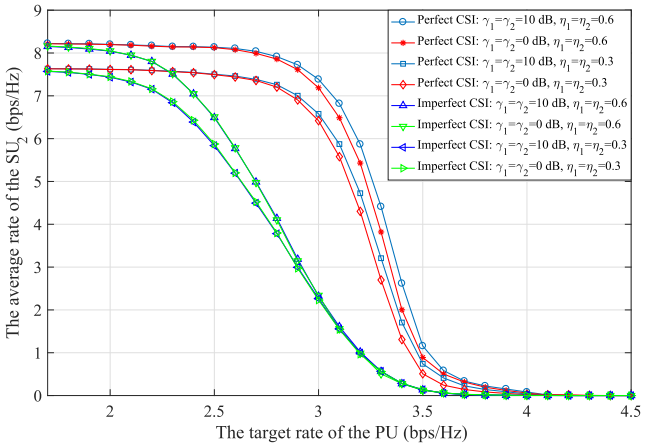

FIGURE 5. The target rate of the PU vs the average rate of the SU_2 with varying energy conversion efficiencies: Comparison between different maximum confidential SINR requirements with perfect and imperfect CSI for $\Gamma_1 = \Gamma_2 = 10$ dBm.

requirements with imperfect CSI is very small, while the performance gap with perfect CSI is relatively large. The imperfect estimation of CSI will introduce additional residual interference to the PU receiver, which cannot be eliminated. Since the maximum confidential SINR requirements of $\gamma_1 = \gamma_2 = 0$ dB are more stringent, the imperfect estimation of CSI has a less impact on the performance of the untrusted secondary system. However, the maximum confidential SINR requirements of $\gamma_1 = \gamma_2 = 10$ dB are more relaxed, and thus the imperfect estimation of CSI has a greater impact on the performance of the untrusted secondary system. Therefore, the performance gap between different maximum confidential SINR requirements with imperfect CSI is not obvious. We can draw a conclusion that the looser the confidential SINR constraints of the untrusted secondary system are, the better performance it can achieve, but the lower the confidentiality of the primary system will be. Similar to Fig. 4, the performance of perfect CSI is always better than

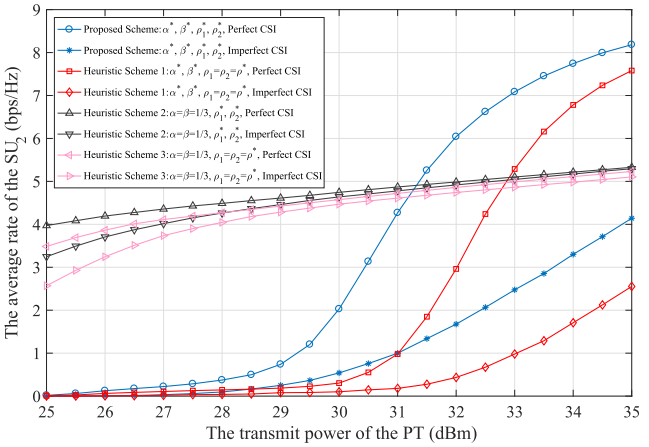

FIGURE 6. The transmit power of the PT vs the average rate of the SU_2: Comparison of different schemes with perfect and imperfect CSI for $\Gamma_1 = \Gamma_2 = 10$ dBm, $\gamma_1 = \gamma_2 = 0$ dB, $\eta_1 = \eta_2 = 0.6$.

that of imperfect CSI, and the performance of the energy conversion efficiencies with $\eta_1 = \eta_2 = 0.6$ is always superior to that with $\eta_1 = \eta_2 = 0.3$.

Fig. 6 shows the performance comparison of different schemes with perfect and imperfect CSI under varying PT rated transmit power. From Fig. 6, we can observe that the average rate of the SU_2 of the heuristic scheme 2 and 3 outperforms that of the proposed scheme and heuristic scheme 1 in the low to medium PT transmit power region. However, for perfect CSI, the average rate of the SU_2 of the proposed scheme and heuristic scheme 1 is superior to that of the other two schemes in the medium to high PT transmit power region. For imperfect CSI, the average rate of the SU_2 of the heuristic scheme 2 and 3 is always superior to that of the other two schemes in the whole PT transmit power region. Since the heuristic scheme 2 and 3 have larger minimum durations than the other two schemes, they can achieve better performance in the low to medium PT transmit power region. As the PT transmit power increase, a shorter duration can satisfy the PU target rate requirement, and thus a remaining longer duration can be utilized to send the untrusted secondary users' data signal which results in better performance.

Fig. 7 shows the impact of the minimum durations on the average rate of the SU_2 with perfect and imperfect CSI under different PT rated transmit power. As can be seen from Fig. 7, when a PT rated transmit power is given, an optimal minimum duration can be determined, which corresponds to the maximum average rate of the SU_2. When the PT rated transmit power is equal to 30 dBm, the maximum average rates of the SU_2 with perfect and imperfect CSI are equal to 6.27 bps/Hz and 5.23 bps/Hz, respectively, which are obviously larger than the average rates corresponding to the heuristic scheme 2 in Fig. 6. Therefore, the proposed scheme is the best by adjusting the minimum durations under different PT rated transmit power.

Fig. 8 demonstrates the performance comparison between different minimum energy harvesting requirements with perfect and imperfect CSI under varying PT rated

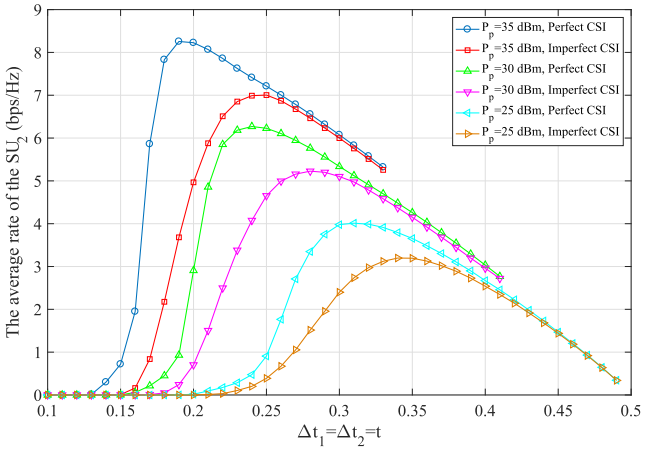

FIGURE 7. The minimum durations of the first two phases vs the average rate of the SU_2: Comparison of different PT rated transmit power with perfect and imperfect CSI for $\Gamma_1 = \Gamma_2 = 10$ dBm, $\gamma_1 = \gamma_2 = 0$ dB, $\eta_1 = \eta_2 = 0.6$.

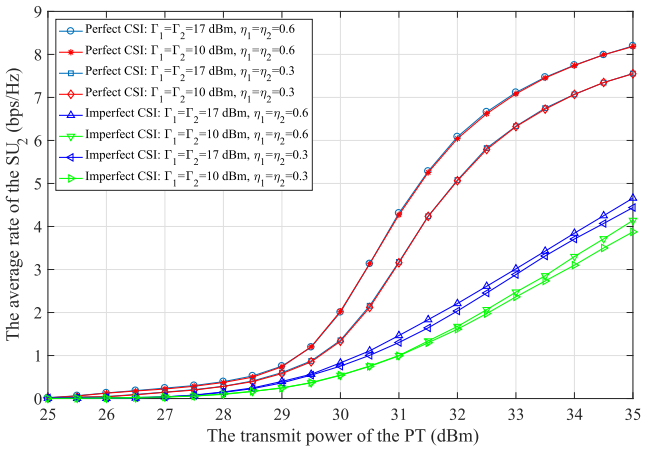

FIGURE 8. The transmit power of the PT vs the average rate of the SU_2 with varying energy conversion efficiencies: Comparison between different minimum energy harvesting requirements with perfect and imperfect CSI for $\gamma_1 = \gamma_2 = 0$ dB.

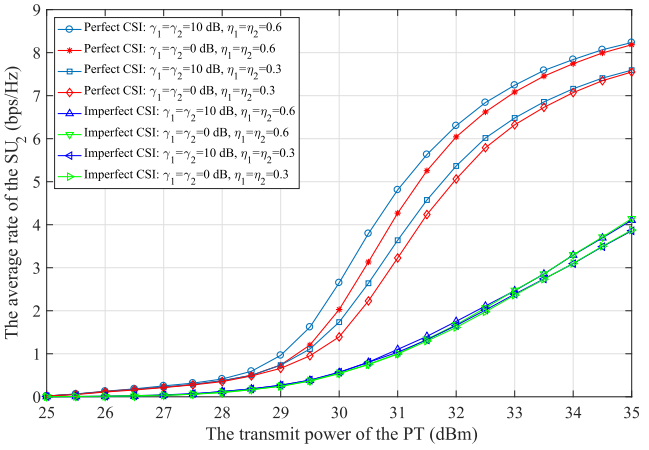

FIGURE 9. The transmit power of the PT vs the average rate of the SU_2 with varying energy conversion efficiencies: Comparison between different maximum confidential SINR requirements with perfect and imperfect CSI for $\Gamma_1 = \Gamma_2 = 10$ dBm.

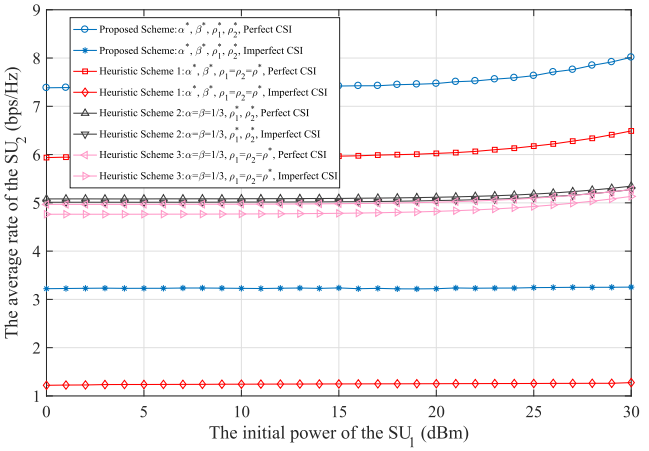

FIGURE 10. The initial power of the SU_1 vs the average rate of the SU_2: Comparison of different schemes with perfect and imperfect CSI for $\Gamma_1 = \Gamma_2 = 10$ dBm, $\gamma_1 = \gamma_2 = 0$ dB, $\eta_1 = \eta_2 = 0.6$.

transmit power. In Fig. 8, as the PT rated transmit power increase, the average rate of the SU_2 also increases. Besides, the average rate of the SU_2 with the minimum energy harvesting requirements $\Gamma_1 = \Gamma_2 = 17$ dBm is superior to that with $\Gamma_1 = \Gamma_2 = 10$ dBm. Similar to Fig. 4, the performance gap between different minimum energy harvesting requirements with perfect CSI is very small, while the performance gap with imperfect CSI is relatively large. We can draw the same conclusion as mentioned in Fig. 4.

The performance comparison between different maximum confidential SINR requirements with perfect and imperfect CSI under varying PT rated transmit power is shown in Fig. 9. With the increase of the PT rated transmit power, the average rate of the SU_2 also increases. In addition, the average rate of the SU_2 with the maximum confidential SINR requirements $\gamma_1 = \gamma_2 = 10$ dB is superior to that with $\gamma_1 = \gamma_2 = 0$ dB. Similar to Fig. 5, the performance gap between different maximum confidential SINR requirements with imperfect CSI is very small, while the performance gap with perfect CSI is relatively large. We can draw the same conclusion as mentioned in Fig. 5.

Fig. 10 shows the performance comparison of different schemes with perfect and imperfect CSI under varying SU_1 initial power. In Fig. 10, for perfect CSI, the average rate of the SU_2 of the proposed scheme is always superior to that of the other three schemes in the whole SU_1 initial power region. For imperfect CSI, the average rate of the SU_2 of the heuristic scheme 2 and 3 is always better than that of the other two schemes in the whole SU_1 initial power region. Furthermore, the performance gap between the proposed scheme and heuristic scheme 1 is relatively large, while the performance gap between the heuristic scheme 2 and 3 is relatively small.

Fig. 11 shows the impact of the minimum durations on the average rate of the SU_2 with perfect and imperfect CSI under different SU_1 initial power. As can be seen from Fig. 11, when a SU_1 initial power is given, an optimal minimum duration can be determined, which corresponds to the maximum

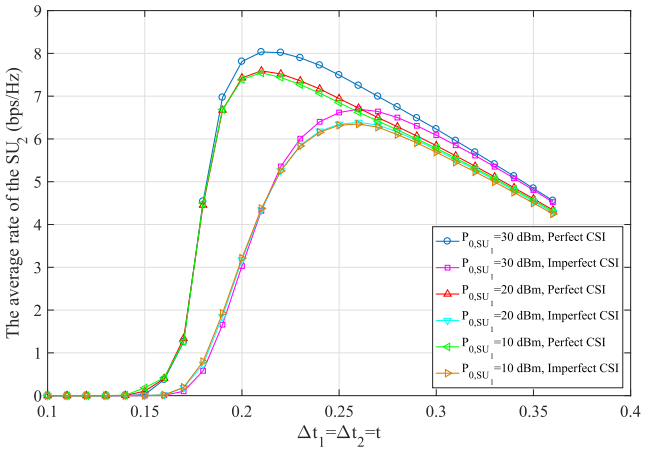

FIGURE 11. The minimum durations of the first two phases vs the average rate of the SU_2: Comparison of different SU_1 initial power with perfect and imperfect CSI for $\Gamma_1 = \Gamma_2 = 10$ dBm, $\gamma_1 = \gamma_2 = 0$ dB, $\eta_1 = \eta_2 = 0.6$.

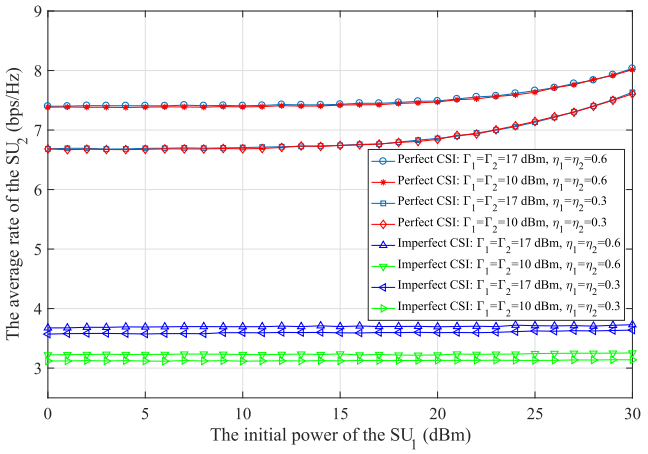

FIGURE 12. The initial power of the SU_1 vs the average rate of the SU_2 with varying energy conversion efficiencies: Comparison between different minimum energy harvesting requirements with perfect and imperfect CSI for $\gamma_1 = \gamma_2 = 0$ dB.

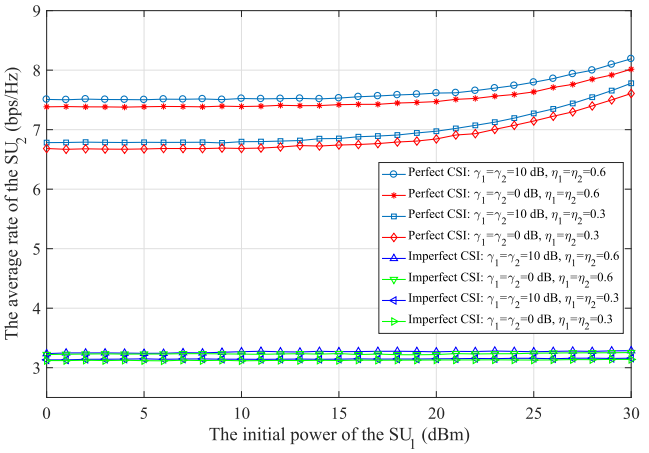

FIGURE 13. The initial power of the SU_1 vs the average rate of the SU_2 with varying energy conversion efficiencies: Comparison between different maximum confidential SINR requirements with perfect and imperfect CSI for $\Gamma_1 = \Gamma_2 = 10$ dBm.

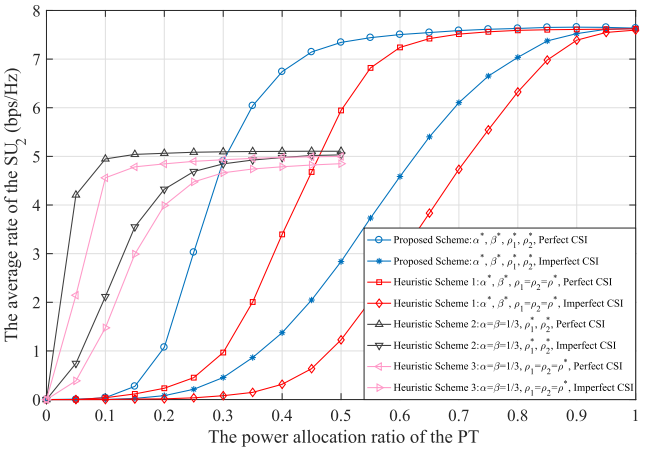

FIGURE 14. The power allocation ratio of the PT vs the average rate of the SU_2: Comparison of different schemes with perfect and imperfect CSI for $\Gamma_1 = \Gamma_2 = 10$ dBm, $\gamma_1 = \gamma_2 = 0$ dB, $\eta_1 = \eta_2 = 0.6$.

average rate of the SU_2. When the SU_1 initial power is equal to 10 dBm, the maximum average rates of the SU_2 with perfect and imperfect CSI are equal to 7.54 bps/Hz and 6.35 bps/Hz, respectively, which are obviously larger than the average rates corresponding to the heuristic scheme 2 in Fig. 10. Therefore, the proposed scheme is the best by adjusting the minimum durations under different SU_1 initial power.

Fig. 12 and Fig. 16 show the performance comparison between different minimum energy harvesting requirements with perfect and imperfect CSI under varying SU_1 initial power and PT power allocation ratios, respectively. In Fig. 12, for perfect CSI, we can observe that with the increase of the SU_1 initial power, the average rate of the SU_2 also increases. However, for imperfect CSI, the average rate of the SU_2 has barely increased. The imperfect estimation of CSI will cause additional residual interference to the PU receiver, and the increase of the SU_1 initial power will compensate its influence so that the performance of the untrusted secondary system is almost unchanged. Therefore, the SU_1 initial power has a less impact on the performance of the untrusted secondary system. Especially for imperfect CSI, the SU_1 initial power has no impact on the system performance. In Fig. 16, as the power allocation ratio of the PT increases, the average rate of the SU_2 is significantly improved in the low to medium PT power allocation ratio region. The more power is allocated to the desired signal, the better assistance that the PU can achieve from the untrusted secondary system, but the lower the confidentiality of the primary system will be. However, for perfect CSI, the average rate of the SU_2 trends to be flat in the medium to high PT power allocation ratio region. Furthermore, from Fig. 12 and Fig. 16, we can draw the same conclusion as mentioned in Fig. 4 and Fig. 8.

Fig. 14 shows the performance comparison of different schemes with perfect and imperfect CSI under varying PT power allocation ratios. From Fig. 14, we can observe that

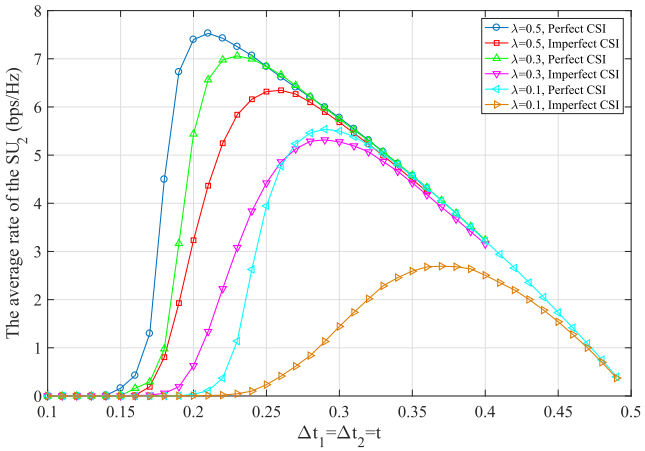

FIGURE 15. The minimum durations of the first two phases vs the average rate of the SU_2: Comparison of different PT power allocation ratios with perfect and imperfect CSI for $\Gamma_1 = \Gamma_2 = 10$ dBm, $\gamma_1 = \gamma_2 = 0$ dB, $\eta_1 = \eta_2 = 0.6$.

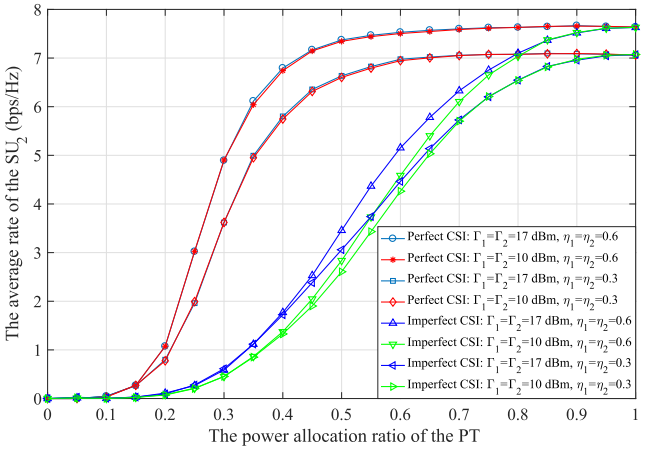

FIGURE 16. The power allocation ratio of the PT vs the average rate of the SU_2 with varying energy conversion efficiencies: Comparison between different minimum energy harvesting requirements with perfect and imperfect CSI for $\gamma_1 = \gamma_2 = 0$ dB.

the average rate of the SU_2 of the heuristic scheme 2 and 3 outperforms that of the other two schemes in the low PT power allocation ratio region. However, the average rate of the SU_2 of the proposed scheme and heuristic scheme 1 is superior to that of the other two schemes in the medium to high PT power allocation ratio region. Since the heuristic scheme 2 and 3 have larger minimum durations than the other two schemes, they can achieve better performance in the low PT power allocation ratio region.

Fig. 15 shows the impact of the minimum durations on the average rate of the SU_2 with perfect and imperfect CSI under different PT power allocation ratios. As can be seen from Fig. 15, when a PT power allocation ratio is given, an optimal minimum duration can be determined, which corresponds to the maximum average rate of the SU_2. When the PT power allocation ratio is equal to 0.1, the maximum average rates of the SU_2 with perfect and imperfect CSI are equal to 5.54 bps/Hz and 2.69 bps/Hz, respectively, which are obviously larger than the average rates corresponding to

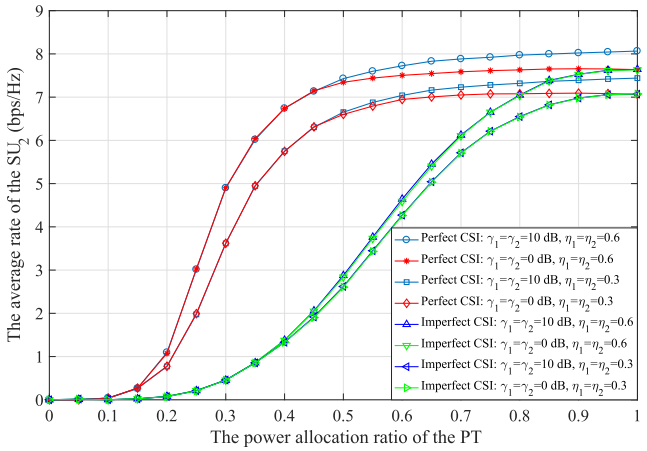

FIGURE 17. The power allocation ratio of the PT vs the average rate of the SU_2 with varying energy conversion efficiencies: Comparison between different maximum confidential SINR requirements with perfect and imperfect CSI for $\Gamma_1 = \Gamma_2 = 10$ dBm.

the heuristic scheme 2 in Fig. 14. Therefore, the proposed scheme is the best by adjusting the minimum durations under different PT power allocation ratios, and it also enables the primary system to achieve better confidentiality.

Fig. 13 and Fig. 17 demonstrate the performance comparison between different maximum confidential SINR requirements with perfect and imperfect CSI under varying SU_1 initial power and PT power allocation ratios, respectively. In Fig. 13, for perfect CSI, with the increase of the SU_1 initial power, the average rate of the SU_2 also increases, but for imperfect CSI, the average rate of the SU_2 has barely increased. Therefore, the SU_1 initial power has a less or no impact on the performance of the untrusted secondary system. In Fig. 17, as the PT power allocation ratio increases, the average rate of the SU_2 is significantly improved in the low to medium PT power allocation ratio region, but for perfect CSI, the average rate of the SU_2 trends to be flat in the medium to high PT power allocation ratio region. Finally, in Fig. 13 and Fig. 17, we can draw the same conclusion as mentioned in Fig. 5 and Fig. 9.

VI. CONCLUSION

This paper proposes a novel AN-aided joint time division- and power splitting-based three-phase secure wireless information and energy cooperation transmission strategy in overlay spectrum sharing networks with untrusted cooperative dual-device-relay. We formulate the optimization problem with the aim to maximize the data rate of the untrusted secondary system, by jointly optimizing the time division ratios, the power splitting ratios, and the beamforming vectors, subject to the PU's target data rate requirement and the untrusted secondary system's maximum power consumption constraints, maximum confidential SINR constraints, and minimum energy harvesting requirements. For practical consideration, this paper not only studies the scenario of perfect CSI but also investigates imperfect CSI

on the impact of the system performance. Simulation results demonstrate that our proposed strategy is the best and significantly improves the average data rate of the untrusted secondary system under different PU target data rate requirements, PT rated transmit power, untrusted SU initial power, and PT power allocation ratios. We can draw the conclusions from simulation results that the more energy the untrusted secondary system harvests, the better performance it can achieve. Furthermore, the looser the confidential SINR constraints of the untrusted secondary system are, the better performance it can achieve, but the lower the confidentiality of the primary system will be. However, by adjusting the minimum durations, our proposed strategy not only significantly improves the average data rate of the untrusted secondary system, but also enables the primary system to achieve better confidentiality. Finally, a large number of simulations show that the time division ratios have a significant impact on the system performance.

APPENDIX A
PROOF OF THEOREM 1

We can easily observe from the optimization problem (20) that the transmit power q_1 can be minimized when its constraints C1 and C2 take the equal sign. Therefore, the constraints C1 and C2 of the optimization problem (20) can be taken the equal sign and replace C2 into C1, and then we can obtain an equation as follows

$$\begin{aligned}&(\rho_1 x_1 - \rho_1\gamma_p N_0 y_1 - \gamma_p N_c y_1)(\sqrt{q_1})^2\\ &+ (\sqrt{\rho_1} z_1 + \sqrt{\rho_1\rho_2 q_2^*}\varphi)\sqrt{q_1} + \sqrt{\rho_2 q_2^*} z_2 + \psi - \gamma_p N_0\\ &+ (\rho_2 x_2 - \rho_2\gamma_p N_0 y_2 - \gamma_p N_c y_2) q_2^* = 0, \end{aligned} \tag{29}$$

where the symbols of the equation (29) are given as follows

$$x_i = \lambda\kappa_i y_i, \quad i \in \{1, 2\}, \tag{30}$$
$$y_i = \|\mathbf{g}_i\|^2 \|\mathbf{h}_i\|^2, \quad i \in \{1, 2\}, \tag{31}$$
$$z_i = 2\lambda\kappa_i \|\mathbf{h}_i\| \mathcal{R}(h), \quad i \in \{1, 2\}, \tag{32}$$
$$q_2^* = \frac{P_{0,\mathrm{SU}_2} + \alpha(1-\rho_2)\xi_2}{\beta(\rho_2\phi_2 + \zeta_2)}, \tag{33}$$
$$\varphi = 2\lambda\kappa_1 \|\mathbf{h}_1\| \|\mathbf{h}_2\| \|\mathbf{g}_2\|^2, \tag{34}$$
$$\psi = \lambda P_p |h|^2. \tag{35}$$

For a given α, β, ρ_i, the formula (29) is a quadratic equation with the variable $\sqrt{q_1}$, so it can be easily solved. The solution of the equation (29) can be expressed as follows

$$q_1^* = \begin{cases} \dfrac{(-b + \sqrt{\Delta})^2}{4a^2}, & \text{for } \Delta > 0 \\ 0, & \text{for } \Delta \le 0 \end{cases} \tag{36}$$

where the symbols of the equation (36) are given as follows

$$a = \rho_1 x_1 - \rho_1\gamma_p N_0 y_1 - \gamma_p N_c y_1 > 0, \tag{37}$$
$$b = \sqrt{\rho_1} z_1 + \sqrt{\rho_1\rho_2 q_2^*}\varphi > 0, \tag{38}$$
$$\begin{aligned} c = {} & (\rho_2 x_2 - \rho_2\gamma_p N_0 y_2 - \gamma_p N_c y_2) q_2^* \\ & + \sqrt{\rho_2 q_2^*} z_2 + \psi - \gamma_p N_0 > 0, \end{aligned} \tag{39}$$
$$\Delta = b^2 - 4ac. \tag{40}$$

According to the C2 constraint of the optimization problem (18), the optimal solution of the transmit power q_s can be expressed as follows

$$q_s^* = \frac{P_{0,\mathrm{SU}_1} + \alpha(1-\rho_1)\xi_1 - \beta(\rho_1\phi_1 + \zeta_1) q_1^*}{1 - \alpha - \beta}. \tag{41}$$

Thus, we have completed the proof of Theorem 1.

APPENDIX B
PROOF OF THEOREM 2

Similar to proof Theorem 1, the constraints C1 and C2 of the optimization problem (27) can be taken the equal sign and replace C2 into C1, and then we can obtain the equation (42), as shown at the bottom of this page, where the symbols of the equation (42) are given as follows

$$\hat{x}_i = \left[\epsilon_i \|\hat{\mathbf{h}}_i\|^2 + 2\sqrt{\epsilon_i(1-\epsilon_i)}\mathcal{R}(\mathbf{e}_i^\dagger \hat{\mathbf{h}}_i)\right] \|\mathbf{g}_i\|^2, \quad i \in \{1, 2\}, \tag{43}$$
$$\hat{y}_i = (1 - \epsilon_i) \frac{|\mathbf{e}_i^\dagger \hat{\mathbf{h}}_i|^2}{\|\hat{\mathbf{h}}_i\|^2} \|\mathbf{g}_i\|^2, \quad i \in \{1, 2\}, \tag{44}$$
$$\hat{z}_i = 2\lambda\kappa_i \left[\sqrt{\epsilon_i} \|\hat{\mathbf{h}}_i\| \mathcal{R}(h) + \frac{\sqrt{1-\epsilon_i}}{\|\hat{\mathbf{h}}_i\|} \mathcal{R}\big(h^\dagger (\mathbf{e}_i^\dagger \hat{\mathbf{h}}_i)\big)\right], \quad i \in \{1, 2\}, \tag{45}$$
$$\hat{q}_2^* = \frac{P_{0,\mathrm{SU}_2} + \alpha(1-\rho_2)\xi_2}{\beta(\rho_2\phi_2 + \zeta_2)}, \tag{46}$$
$$\hat{\varphi}_1 = 2\lambda\kappa_1 \|\mathbf{g}_2\|^2 \sqrt{\epsilon_1\epsilon_2} \|\hat{\mathbf{h}}_1\| \|\hat{\mathbf{h}}_2\|, \tag{47}$$
$$\hat{\varphi}_2 = 2\lambda\kappa_1 \|\mathbf{g}_2\|^2 \sqrt{\epsilon_1(1-\epsilon_2)} \frac{\|\hat{\mathbf{h}}_1\|}{\|\hat{\mathbf{h}}_2\|} \mathcal{R}(\mathbf{e}_2^\dagger \hat{\mathbf{h}}_2), \tag{48}$$
$$\hat{\varphi}_3 = 2\lambda\kappa_1 \|\mathbf{g}_2\|^2 \sqrt{(1-\epsilon_1)\epsilon_2} \frac{\|\hat{\mathbf{h}}_2\|}{\|\hat{\mathbf{h}}_1\|} \mathcal{R}(\hat{\mathbf{h}}_1^\dagger \mathbf{e}_1), \tag{49}$$
$$\hat{\varphi}_4 = 2\lambda\kappa_1 \|\mathbf{g}_2\|^2 \frac{\sqrt{(1-\epsilon_1)(1-\epsilon_2)}}{\|\hat{\mathbf{h}}_1\| \|\hat{\mathbf{h}}_2\|} \mathcal{R}(\hat{\mathbf{h}}_1^\dagger \mathbf{e}_1 \mathbf{e}_2^\dagger \hat{\mathbf{h}}_2). \tag{50}$$

For a given α, β, ρ_i, the formula (42) is a quadratic equation with the variable $\sqrt{\hat{q}_1}$, so it can be easily solved. The solution

$$\begin{aligned}&\left[(\rho_1\lambda\kappa_1 - \rho_1\gamma_p N_0 - \gamma_p N_c)\hat{x}_1 + (\rho_1\lambda\kappa_1 - \rho_1\gamma_p\vartheta_1 - \gamma_p N_c)\hat{y}_1\right](\sqrt{\hat{q}_1})^2 + \left[\sqrt{\rho_1}\hat{z}_1 + \sqrt{\rho_1\rho_2\hat{q}_2^*}(\hat{\varphi}_1 + \hat{\varphi}_2 + \hat{\varphi}_3 + \hat{\varphi}_4)\right]\sqrt{\hat{q}_1}\\ &+ \left[(\rho_2\lambda\kappa_2 - \rho_2\gamma_p N_0 - \gamma_p N_c)\hat{x}_2 + (\rho_2\lambda\kappa_2 - \rho_2\gamma_p\vartheta_2 - \gamma_p N_c)\hat{y}_2\right]\hat{q}_2^* + \sqrt{\rho_2\hat{q}_2^*}\hat{z}_2 + \psi - \gamma_p N_0 = 0, \end{aligned} \tag{42}$$

of the equation (42) can be expressed as follows

$$\hat{q}_1^* = \begin{cases} \dfrac{(-\hat{b}+\sqrt{\hat{\Delta}})^2}{4\hat{a}^2}, & \text{for } \hat{\Delta} > 0 \\ 0, & \text{for } \hat{\Delta} \le 0 \end{cases} \tag{51}$$

where the symbols of the equation (51) are given as follows

$$\begin{aligned} \hat{a} &= (\rho_1\lambda\kappa_1 - \rho_1\gamma_p N_0 - \gamma_p N_c)\hat{x}_1 \\ &\quad + (\rho_1\lambda\kappa_1 - \rho_1\gamma_p\vartheta_1 - \gamma_p N_c)\hat{y}_1 > 0, \qquad (52) \\ \hat{b} &= \sqrt{\rho_1}\hat{z}_1 + \sqrt{\rho_1\rho_2\hat{q}_2^*}(\hat{\varphi}_1 + \hat{\varphi}_2 + \hat{\varphi}_3 + \hat{\varphi}_4) > 0, \qquad (53) \\ \hat{c} &= \Big[(\rho_2\lambda\kappa_2 - \rho_2\gamma_p N_0 - \gamma_p N_c)\hat{x}_2 \\ &\quad + (\rho_2\lambda\kappa_2 - \rho_2\gamma_p\vartheta_2 - \gamma_p N_c)\hat{y}_2\Big]\hat{q}_2^* \\ &\quad + \sqrt{\rho_2\hat{q}_2^*}\hat{z}_2 + \psi - \gamma_p N_0 > 0, \qquad (54) \\ \hat{\Delta} &= \hat{b}^2 - 4\hat{a}\hat{c}. \qquad (55) \end{aligned}$$

According to the C2 constraint of the optimization problem (18), the optimal solution of the transmit power $\hat{q}_s$ can be expressed as follows

$$\hat{q}_s^* = \frac{P_{0,\mathrm{SU}_1} + \alpha(1-\rho_1)\xi_1 - \beta(\rho_1\phi_1 + \zeta_1)\hat{q}_1^*}{1-\alpha-\beta}. \tag{56}$$

Thus, we have completed the proof of Theorem 2.

REFERENCES

[1] L. Gavrilovska, D. Denkovski, V. Rakovic, and M. Angjelichinoski, "Medium access control protocols in cognitive radio networks: Overview and general classification," *IEEE Commun. Surveys Tuts.*, vol. 16, no. 4, pp. 2092–2124, 4th Quart., 2014.

[2] W. Liang, S. X. Ng, and L. Hanzo, "Cooperative overlay spectrum access in cognitive radio networks," *IEEE Commun. Surveys Tuts.*, vol. 19, no. 3, pp. 1924–1944, 3rd Quart., 2017.

[3] M. R. Hassan, G. C. Karmakar, J. Kamruzzaman, and B. Srinivasan, "Exclusive use spectrum access trading models in cognitive radio networks: A survey," *IEEE Commun. Surveys Tuts.*, vol. 19, no. 4, pp. 2192–2231, 4th Quart., 2017.

[4] X. Lu, P. Wang, D. Niyato, and E. Hossain, "Dynamic spectrum access in cognitive radio networks with RF energy harvesting," *IEEE Wireless Commun.*, vol. 21, no. 3, pp. 102–110, Jun. 2014.

[5] L. Mohjazi, M. Dianati, G. K. Karagiannidis, S. Muhaidat, and M. Al-Qutayri, "RF-powered cognitive radio networks: Technical challenges and limitations," *IEEE Commun. Mag.*, vol. 53, no. 4, pp. 94–100, Apr. 2015.

[6] X. Chen, Z. Zhang, H.-H. Chen, and H. Zhang, "Enhancing wireless information and power transfer by exploiting multi-antenna techniques," *IEEE Commun. Mag.*, vol. 53, no. 4, pp. 133–141, Apr. 2015.

[7] X. Lu, P. Wang, D. Niyato, D. I. Kim, and Z. Han, "Wireless networks with RF energy harvesting: A contemporary survey," *IEEE Commun. Surveys Tuts.*, vol. 17, no. 2, pp. 757–789, 2nd Quart., 2015.

[8] X. Huang, T. Han, and N. Ansari, "On green-energy-powered cognitive radio networks," *IEEE Commun. Surveys Tuts.*, vol. 17, no. 2, pp. 827–842, 2nd Quart., 2015.

[9] Y. Liu, H.-H. Chen, and L. Wang, "Physical layer security for next generation wireless networks: Theories, technologies, and challenges," *IEEE Commun. Surveys Tuts.*, vol. 19, no. 1, pp. 347–376, 1st Quart., 2017.

[10] X. Chen, D. W. K. Ng, W. H. Gerstacker, and H.-H. Chen, "A survey on multiple-antenna techniques for physical layer security," *IEEE Commun. Surveys Tuts.*, vol. 19, no. 2, pp. 1027–1053, 2nd Quart., 2017.

[11] Y. Wu, A. Khisti, C. Xiao, G. Caire, K.-K. Wong, and X. Gao, "A survey of physical layer security techniques for 5G wireless networks and challenges ahead," *IEEE J. Sel. Areas Commun.*, vol. 36, no. 4, pp. 679–695, Apr. 2018.

[12] Q. Li, Q. Zhang, and J. Qin, "Beamforming in non-regenerative two-way multi-antenna relay networks for simultaneous wireless information and power transfer," *IEEE Trans. Wireless Commun.*, vol. 13, no. 10, pp. 5509–5520, Oct. 2014.

[13] Q. Li, Q. Zhang, and J. Qin, "Robust Tomlinson–Harashima precoding with Gaussian uncertainties for SWIPT in MIMO broadcast channels," *IEEE Trans. Signal Process.*, vol. 65, no. 6, pp. 1399–1411, Mar. 2017.

[14] Q. Li and L. Yang, "Robust optimization for energy efficiency in MIMO two-way relay networks with SWIPT," *IEEE Syst. J.*, to be published.

[15] G. Zheng, Z. Ho, E. A. Jorswieck, and B. Ottersten, "Information and energy cooperation in cognitive radio networks," *IEEE Trans. Signal Process.*, vol. 62, no. 9, pp. 2290–2303, May 2014.

[16] S. Yin, E. Zhang, Z. Qu, L. Yin, and S. Li, "Optimal cooperation strategy in cognitive radio systems with energy harvesting," *IEEE Trans. Wireless Commun.*, vol. 13, no. 9, pp. 4693–4707, Sep. 2014.

[17] Q. Gao, T. Jing, X. Xing, X. Cheng, Y. Huo, and D. Chen, "Simultaneous energy and information cooperation in MIMO cooperative cognitive radio systems," in *Proc. IEEE Wireless Commun. Netw. Conf. (WCNC)*, Mar. 2015, pp. 351–356.

[18] J. J. Pradha, S. S. Kalamkar, and A. Banerjee, "On information and energy cooperation in energy harvesting cognitive radio," in *Proc. IEEE 26th Annu. Int. Symp. Pers., Indoor, Mobile Radio Commun. (PIMRC)*, Aug. 2015, pp. 943–948.

[19] Z. Gao and B. Wang, "User cooperation in OFDM-based cognitive radio networks with simultaneous wireless information and power transfer," in *Proc. Int. Conf. Wireless Commun. Signal Process. (WCSP)*, Oct. 2015, pp. 1–6.

[20] D. Zhao, Y. Cui, H. Tian, and P. Zhang, "A novel information and energy cooperation transmission scheme in cognitive spectrum sharing-based D2D communication systems," *IEEE Access*, vol. 7, pp. 72316–72328, May 2019.

[21] S. Lee and R. Zhang, "Cognitive wireless powered network: Spectrum sharing models and throughput maximization," *IEEE Trans. Cognit. Commun. Netw.*, vol. 1, no. 3, pp. 335–346, Sep. 2015.

[22] J. Kim, H. Lee, C. Song, T. Oh, and I. Lee, "Sum throughput maximization for multi-user MIMO cognitive wireless powered communication networks," *IEEE Trans. Wireless Commun.*, vol. 16, no. 2, pp. 913–923, Feb. 2017.

[23] Y. Liu, S. A. Mousavifar, Y. Deng, C. Leung, and M. Elkashlan, "Wireless energy harvesting in a cognitive relay network," *IEEE Trans. Wireless Commun.*, vol. 15, no. 4, pp. 2498–2508, Apr. 2016.

[24] M. Sami, N. K. Noordin, and M. Khabazian, "A TDMA-based cooperative MAC protocol for cognitive networks with opportunistic energy harvesting," *IEEE Commun. Lett.*, vol. 20, no. 4, pp. 808–811, Apr. 2016.

[25] C. Zhai, J. Liu, and L. Zheng, "Relay-based spectrum sharing with secondary users powered by wireless energy harvesting," *IEEE Trans. Commun.*, vol. 64, no. 5, pp. 1875–1887, May 2016.

[26] K.-Y. Hsieh, F.-S. Tseng, and M.-L. Ku, "A spectrum and energy cooperation strategy in hierarchical cognitive radio cellular networks," *IEEE Wireless Commun. Lett.*, vol. 5, no. 3, pp. 252–255, Jun. 2016.

[27] Q. Li, Q. Zhang, and J. Qin, "Beamforming for information and energy cooperation in cognitive non-regenerative two-way relay networks," *IEEE Trans. Wireless Commun.*, vol. 15, no. 8, pp. 5302–5313, Aug. 2016.

[28] Z. Xie, Q. Zhu, and S. Zhao, "Resource allocation algorithm based on energy cooperation in two-way cognitive radio relay networks," in *Proc. Int. Conf. Wireless Commun. Signal Process. (WCSP)*, Oct. 2017, pp. 1–7.

[29] S. Yin, Z. Qu, Z. Wang, and L. Li, "Energy-efficient cooperation in cognitive wireless powered networks," *IEEE Commun. Lett.*, vol. 21, no. 1, pp. 128–131, Jan. 2017.

[30] H. Xing, X. Kang, K.-K. Wong, and A. Nallanathan, "Optimizing DF cognitive radio networks with full-duplex-enabled energy access points," *IEEE Trans. Wireless Commun.*, vol. 16, no. 7, pp. 4683–4697, Jul. 2017.

[31] W. Xu, Z. Liu, S. Li, and J. Lin, "Two-plus-one cognitive cooperation based on energy harvesting and spatial multiplexing," *IEEE Trans. Veh. Technol.*, vol. 66, no. 8, pp. 7589–7593, Aug. 2017.

[32] J. He, S. Guo, G. Pan, Y. Yang, and D. Liu, "Relay cooperation and outage analysis in cognitive radio networks with energy harvesting," *IEEE Syst. J.*, vol. 12, no. 3, pp. 2129–2140, Sep. 2018.

[33] Z. Zhu, Z. Chu, Z. Wang, and I. Lee, "Outage constrained robust beamforming for secure broadcasting systems with energy harvesting," *IEEE Trans. Wireless Commun.*, vol. 15, no. 11, pp. 7610–7620, Nov. 2016.

[34] Z. Zhu, Z. Chu, N. Wang, S. Huang, Z. Wang, and I. Lee, "Beamforming and power splitting designs for AN-aided secure multi-user MIMO SWIPT systems," *IEEE Trans. Inf. Forensics Security*, vol. 12, no. 12, pp. 2861–2874, Dec. 2017.
[35] Z. Zhu, Z. Chu, F. Zhou, H. Niu, Z. Wang, and I. Lee, "Secure beamforming designs for secrecy MIMO SWIPT systems," *IEEE Wireless Commun. Lett.*, vol. 7, no. 3, pp. 424–427, Jun. 2018.
[36] Q. Li and L. Yang, "Beamforming for cooperative secure transmission in cognitive two-way relay networks," *IEEE Trans. Inf. Forensics Security*, to be published.
[37] B. Fang, Z. Qian, W. Zhong, and W. Shao, "An-aided secrecy precoding for SWIPT in cognitive MIMO broadcast channels," *IEEE Commun. Lett.*, vol. 19, no. 9, pp. 1632–1635, Sep. 2015.
[38] T. Zhang, Y. Huang, Y. Cai, and W. Yang, "Secure transmission in spectrum sharing relaying networks with multiple antennas," *IEEE Commun. Lett.*, vol. 20, no. 4, pp. 824–827, Apr. 2016.
[39] Y. Huang, Z. Li, F. Zhou, and R. Zhu, "Robust AN-aided beamforming design for secure MISO cognitive radio based on a practical nonlinear EH model," *IEEE Access*, vol. 5, pp. 14011–14019, Aug. 2017.
[40] P. Yan, Y. Zou, and J. Zhu, "Energy-aware multiuser scheduling for physical-layer security in energy-harvesting underlay cognitive radio systems," *IEEE Trans. Veh. Technol.*, vol. 67, no. 3, pp. 2084–2096, Mar. 2018.
[41] D. Chen, Y. Cheng, W. Yang, J. Hu, and Y. Cai, "Physical layer security in cognitive untrusted relay networks," *IEEE Access*, vol. 6, pp. 7055–7065, Oct. 2017.
[42] L. Jiang, H. Tian, C. Qin, S. Gjessing, and Y. Zhang, "Secure beamforming in wireless-powered cooperative cognitive radio networks," *IEEE Commun. Lett.*, vol. 20, no. 3, pp. 522–525, Mar. 2016.
[43] Y. Wu and X. Chen, "Robust beamforming and power splitting for secrecy wireless information and power transfer in cognitive relay networks," *IEEE Commun. Lett.*, vol. 20, no. 6, pp. 1152–1155, Jun. 2016.
[44] M. Zhang and Y. Liu, "Secure beamforming for untrusted MISO cognitive radio networks," *IEEE Trans. Wireless Commun.*, vol. 17, no. 7, pp. 4861–4872, Jul. 2018.
[45] R. Zhang and C. K. Ho, "MIMO broadcasting for simultaneous wireless information and power transfer," *IEEE Trans. Wireless Commun.*, vol. 12, no. 5, pp. 1989–2001, May 2013.
[46] H. Xing, L. Liu, and R. Zhang, "Secrecy wireless information and power transfer in fading wiretap channel," *IEEE Trans. Veh. Technol.*, vol. 65, no. 1, pp. 180–190, Jan. 2016.
[47] M. Zhang, Y. Liu, and R. Zhang, "Artificial noise aided secrecy information and power transfer in OFDMA systems," *IEEE Trans. Wireless Commun.*, vol. 15, no. 4, pp. 3085–3096, Apr. 2016.
[48] A. Mabrouk, A. El Shafie, K. Tourki, and N. Al-Dhahir, "AN-aided relay-selection scheme for securing untrusted RF-EH relay systems," *IEEE Trans. Green Commun. Netw.*, vol. 1, no. 4, pp. 481–493, Dec. 2017.
[49] H. Koorapaty, A. A. Hassan, and S. Chennakeshu, "Secure information transmission for mobile radio," *IEEE Commun. Lett.*, vol. 4, no. 2, pp. 52–55, Feb. 2000.
[50] Q. Wang, H. Su, K. Ren, and K. Kim, "Fast and scalable secret key generation exploiting channel phase randomness in wireless networks," in *Proc. IEEE Int. Conf. Comput. Commun. (INFOCOM)*, Apr. 2011, pp. 1422–1430.
[51] D. W. K. Ng, E. S. Lo, and R. Schober, "Robust beamforming for secure communication in systems with wireless information and power transfer," *IEEE Trans. Wireless Commun.*, vol. 13, no. 8, pp. 4599–4615, Aug. 2014.
[52] G. Zheng, S. Song, K.-K. Wong, and B. Ottersten, "Cooperative cognitive networks: Optimal, distributed and low-complexity algorithms," *IEEE Trans. Signal Process.*, vol. 61, no. 11, pp. 2778–2790, Jun. 2013.
[53] A. Goldsmith, *Wireless Communications*. Cambridge, U.K.: Cambridge Univ. Press, 2005.
[54] MathWorks. *Fmincon Interior Point Algorithm*. Accessed: Jul. 6, 2019. [Online]. Available: https://www.mathworks.com/help/optim/ug/constrained-nonlinear-optimization-algorithms.html#brnpd5f
[55] R. A. Waltz, J. L. Morales, J. Nocedal, and D. Orban, "An interior algorithm for nonlinear optimization that combines line search and trust region steps," *Math. Program.*, vol. 107, no. 3, pp. 391–408, 2006.
[56] S. Boyd and L. Vandenberghe, *Convex Optimization*. Cambridge, U.K.: Cambridge Univ. Press, 2004.

DAQIAN ZHAO received the M.S. degree in information and communication engineering from the Chongqing University of Posts and Telecommunications, China, in 2014. He is currently pursuing the Ph.D. degree with the Beijing University of Posts and Telecommunications, China. His research interests include cognitive radio networks, cooperative communication, wireless information and power transfer, and physical layer security.

HUI TIAN received the M.S. degree in microelectronics and the Ph.D. degree in circuits and systems from the Beijing University of Posts and Telecommunications, China, in 1992 and 2003, respectively, where she is currently a Professor, the Director of the State Key Laboratory of Networking and Switching Technology, Network Information Processing Research Center, and the MAT Director of the Wireless Technology Innovation Institute. Her current research interests mainly include radio resource management, cross-layer optimization, M2M, cooperative communication, mobile social networks, and mobile edge computing.

PING ZHANG received the M.S. degree in electrical engineering from Northwestern Polytechnical University, China, in 1986, and the Ph.D. degree in electric circuits and systems from the Beijing University of Posts and Telecommunications, China, in 1990, where he is currently a Professor and the Director of the State Key Laboratory of Networking and Switching Technology.

He is a member of next-generation broadband wireless communication network of the National Science and Technology Major Project. His research interests include broadband wireless communication, new technologies on cognitive wireless networks, TD-LTE, multiple-input-multiple-output (MIMO), and OFDM. He is a member of the Fifth Advisory Committee of the National Natural Science Foundation of China and the 11th Beijing Municipal Committee of the Chinese People's Political Consultative Conference. He is also the Chief Scientist of the 973 National Basic Research Program of China and the Owner of the Special Government Allowance of the State Council of China. He was a recipient of the First and Second Prizes of the National Technology Invention and Technological Progress Awards and the First Prize of the Outstanding Achievement Award of Scientific Research in College. He has received the Second Award for the National Science and Technology Prize, twice, the Second Award for the National Science and Technology Invention Prize, once, the Provincial Science and Technology Awards, many times, and the Title of Outstanding Science and Technological Workers, in 2010. He is also the Executive Associate Editor-in-Chief of *Information Sciences* and *Chinese Science Bulletin*, a Guest Editor of the *IEEE Wireless Communications Magazine*, and an Editor of *China Communications*.